

## ORIGINAL ARTICLE

**Systemic administration of IL-33 induces a population of circulating KLRG1<sup>hi</sup> type 2 innate lymphoid cells and inhibits type 1 innate immunity against multiple myeloma**Camille Guillerey<sup>1,2</sup> , Kimberley Stannard<sup>1</sup>, Jason Chen<sup>1,2</sup>, Sophie Krumeich<sup>1</sup>, Kim Miles<sup>1</sup>, Kyohei Nakamura<sup>1</sup> , Jessica Smith<sup>1,3</sup>, Yuan Yu<sup>1</sup>, Susanna Ng<sup>4</sup> , Heidi Harjunpää<sup>2,5</sup>, Michele WL Teng<sup>5</sup>, Christian Engwerda<sup>4</sup>, Gabrielle T Belz<sup>6</sup> & Mark J Smyth<sup>1,2</sup> 

1 Immunology in Cancer and Infection Laboratory, QIMR Berghofer Medical Research Institute, Herston, QLD, Australia

2 School of Medicine, The University of Queensland, Herston, QLD, Australia

3 School of Environment and Sciences, Griffith University, Brisbane, QLD, Australia

4 Immunology and Infection Laboratory, QIMR Berghofer Medical Research Institute, Herston, QLD, Australia

5 Cancer Immunoregulation and Immunotherapy Laboratory, QIMR Berghofer Medical Research Institute, Herston, QLD, Australia

6 Immunology Division, Walter and Eliza Hall Institute of Medical Research, Parkville, Melbourne, VIC, Australia

**Keywords**

Cancer immunology, cytokine, IL-33, immunotherapy, innate immunity, innate lymphoid cells, multiple myeloma

**Correspondence**Camille Guillerey, Cancer Immunotherapies Laboratory, Mater Research Institute, The University of Queensland, Translational Research Institute, Woolloongabba, Brisbane, QLD 4101, Australia.  
E-mail: camille.guillerey@mater.uq.edu.au**Present address**

Camille Guillerey, Cancer Immunotherapies Laboratory, Mater Research Institute, The University of Queensland, Translational Research Institute, Woolloongabba, Brisbane, QLD, Australia

Received 24 March 2020; Revised 30 July 2020; Accepted 30 July 2020

doi: 10.1111/imcb.12390

*Immunology & Cell Biology* 2021; 99: 65–83**Abstract**

Type 2 innate lymphoid cells (ILC2s) are important producers of type 2 cytokines whose role in hematological cancers remains unclear. ILC2s are a heterogeneous population encompassing distinct subsets with different tissue localization and cytokine responsiveness. In this study, we investigated the role of bone marrow (BM) ILC2s and interleukin (IL)-33-stimulated ILC2s in multiple myeloma, a plasma cell malignancy that develops in the BM. We found that myeloma growth was associated with phenotypic and functional alterations of BM ILC2s, characterized by an increased expression of maturation markers and reduced cytokine response to IL-2/IL-33. We identified a population of KLRG1<sup>hi</sup> ILC2s that preferentially accumulated in the liver and spleen of *Il2rg*<sup>-/-</sup> *Rag2*<sup>-/-</sup> mice reconstituted with BM ILC2s. A similar population of KLRG1<sup>hi</sup> ILC2s was observed in the blood, liver and spleen of IL-33-treated wild-type mice. The presence of KLRG1<sup>hi</sup> ILC2s in ILC2-reconstituted *Il2rg*<sup>-/-</sup> *Rag2*<sup>-/-</sup> mice or in IL-33-treated wild-type mice was associated with increased eosinophil numbers but had no effect on myeloma progression. Interestingly, while decreased myeloma growth was observed following treatment of Rag-deficient mice with the type 1 cytokines IL-12 and IL-18, this protection was reversed when mice received a combined treatment of IL-33 together with IL-12 and IL-18. In summary, our data indicate that IL-33 treatment induces a population of circulating inflammatory KLRG1<sup>hi</sup> ILC2s and inhibits type 1 immunity against multiple myeloma. These results argue against therapeutic administration of IL-33 to myeloma patients.

**INTRODUCTION**

Innate lymphoid cells (ILCs) are a group of developmentally related immune cells that integrate multiple pathogen and host-derived signals to ensure tissue homeostasis and provide early protection against infections.<sup>1</sup> Type 2 ILCs (ILC2s) are considered innate counterparts of T-helper 2 cells and are dependent on

the transcription factors GATA3 and ROR $\alpha$ .<sup>2</sup> ILC2s respond to epithelium-derived alarmins [i.e. interleukin (IL)-25, IL-33 and thymic stromal lymphopoietin (TSLP)] by releasing high levels of type 2 cytokines such as IL-5 and IL-13. While ILC2s are well known for their contribution to allergic asthma and to anti-helminth immunity,<sup>3</sup> their role in cancer is only beginning to be revealed.<sup>4,5</sup>

Both tumor-suppressive and tumor-promoting activities of ILC2s have been described. ILC2s appear to facilitate immune escape by promoting the accumulation of myeloid-derived suppressor cells<sup>6,7</sup> and by downregulating natural killer (NK) cell functions.<sup>8</sup> However, other studies indicated a protective role for ILC2s in mouse cancer models engineered to produce high levels of IL-33,<sup>9,10</sup> and mouse ILC2-induced eosinophilia was found to protect against experimental lung metastasis.<sup>11</sup> Moreover, a recent study reported a protective role of ILC2s in mouse and human pancreatic tumors.<sup>12</sup> The reasons for these discrepancies remain unclear and a deeper knowledge of ILC2 biology is needed to fully understand their role in cancer.

It has now become evident that ILC2s are not a homogenous population, but that distinct ILC2 subsets can be defined based on their phenotype, localization and function. For instance, ILC2s from different tissues exhibit distinct patterns of cytokine responsiveness; lung ILC2s are activated by IL-33,<sup>13</sup> whereas intestinal ILC2s respond primarily to IL-25,<sup>14</sup> and skin ILC2s respond to TSLP and IL-18.<sup>15,16</sup> Heterogeneity of ILC2s was observed within a given tissue as single-cell transcriptomic analyses compartmentalized mouse small intestine ILC2s into four sub-subsets.<sup>17</sup> Moreover, two distinct populations termed “natural” and “inflammatory” ILC2s have been defined in mice,<sup>18,19</sup> and memory-like ILC2s have been observed in the mouse lung and mediastinal lymph nodes.<sup>13</sup> ILC2 plasticity and their ability to differentiate into interferon- $\gamma$  (IFN $\gamma$ )-producing ILC1s, or IL-17-producing ILC3s further complicate the picture.<sup>18,20–22</sup>

IL-33 is a potent activator of ILC2s that recently gained attention in the field of tumor immunity.<sup>23</sup> The ability of IL-33 to promote type 1 immune responses,<sup>24</sup> including NK cell activity,<sup>25,26</sup> to reduce the suppressive activity of myeloid-derived suppressor cells<sup>27</sup> and to overcome immune tolerance<sup>28</sup> supports the idea that IL-33 might represent a suitable adjuvant for cancer immunotherapy.<sup>29</sup> However, the pleiotropic activity of IL-33 on cancer cells as well as on immune and stroma cells within the tumor microenvironment may also foster tumor progression.<sup>30</sup> Therefore, therapeutic application of IL-33 in cancer warrants further investigation.

In this study, we investigated the role of ILC2s in multiple myeloma (MM), a blood cancer developing in the bone marrow (BM). Since a population of immature ILC2s has been described in the mouse BM,<sup>31,32</sup> we asked whether BM ILC2s play a role in immune responses to MM. Moreover, given the importance of type 1 immune responses in myeloma control,<sup>33,34</sup> it was necessary to define whether IL-33 could enhance these responses, as previously suggested in other models.<sup>24–26</sup> We analyzed the response of BM ILC2s to systemic injection of IL-33

and asked whether ILC2 plasticity could be harnessed to promote type 1 immunity in the context of blood cancer. Our data identified a population of blood-circulating KLRG1<sup>hi</sup> ILC2s that could be derived from BM ILC2s and preferentially accumulated in the liver of IL-33-treated mice. While the presence of these KLRG1<sup>hi</sup> ILC2s had no effect on myeloma progression in the absence of additional treatment, our work argues against a clinical use of IL-33 in cancer patients because systemic administration of this cytokine abolished the anti-myeloma activity of IL-12 and IL-18 immunotherapy.

## RESULTS

### BM ILC2s and peripheral mature ILC2s exhibit different phenotypes

Published reports have used different markers to characterize ILC2s and high heterogeneity of ILC2 populations has been reported between different organs.<sup>16</sup> Differences between male and female ILC2s have also been reported.<sup>35</sup> Therefore, we first aimed to define the phenotype of BM ILC2s in naïve mice. For this, we compared BM ILC2s with mature ILC2s from the lung and mesenteric lymph nodes of both male and female mice. In agreement with established mouse ILC2 markers,<sup>36</sup> ILC2s were defined as Lin<sup>-</sup>ID2<sup>+</sup>CD127<sup>+</sup>CD25<sup>+</sup> lymphocytes in *Id2*<sup>GFP/GFP</sup> mice, or alternatively as Lin<sup>-</sup>CD127<sup>+</sup>CD25<sup>+</sup>ST2<sup>+</sup> lymphocytes in the absence of ID2 reporter (Supplementary figures 1 and 2a). Using female *Id2*<sup>GFP/GFP</sup> mice, we observed that, in contrast to lung and mesenteric lymph node ILC2s, BM ILC2s were uniformly ST2<sup>hi</sup> and Scal<sup>hi</sup> and expressed low levels of KLRG1 and CD117 (Supplementary figures 2b and c). In agreement with previous reports,<sup>35,37,38</sup> we observed a higher percentage of KLRG1<sup>+</sup> ILC2s in the lung and BM of male mice, compared with female mice (Supplementary figures 2d and e). However, no differences between sexes were observed in the mesenteric lymph nodes. To investigate the function of KLRG1<sup>+</sup> and KLRG1<sup>-</sup> ILC2 subsets, we sorted these two subsets from the BM of male *Id2*<sup>GFP/GFP</sup> mice and cultured them in the presence of IL-2 and IL-33. We found that, under these conditions, KLRG1<sup>+</sup> ILC2s produced more IL-5, IL-6 and IL-13 than KLRG1<sup>-</sup> ILC2s (Supplementary figure 2f). KLRG1<sup>+</sup> and KLRG1<sup>-</sup> ILC2 subsets expressed similar levels of IL-2 receptor  $\alpha$  (CD25) and IL-33 receptor (ST2), suggesting that functional differences between these two subsets were not caused by different responsiveness to IL-2 or IL-33 (Supplementary figure 2g). Collectively, these data highlight phenotypic differences between ILC2s in relation to their organ localization and indicate functional differences between KLRG1<sup>+</sup> and KLRG1<sup>-</sup> ILC2 subsets at steady state.

### MM development in the BM is associated with subtle modifications of ILC2 phenotype and decreased function

To characterize the response of BM ILC2s to tumors, we challenged mice with the Vk\*MYC myeloma cell line Vk12653.<sup>34</sup> In this model, MM develops slowly and malignant plasma cells become readily detectable in the BM 2–3 weeks after Vk12653 cell challenge.<sup>33</sup> At later stages of disease, Vk\*MYC myeloma cells colonize the spleen and liver. First, we assessed whether the presence of myeloma cells in the BM altered the potential of cells in this tissue to produce cytokines. We measured cytokine levels in culture supernatants from bulk BM cells obtained from naïve and MM-bearing mice at week 5 post-Vk\*MYC myeloma cell inoculation. We observed a small increase in TSLP levels in the BM of MM-bearing mice (Supplementary figure 3a). By contrast, IL-25 levels were decreased in the presence of MM (Supplementary figure 3b) and we could not detect IL-33 in the culture supernatants from BM cells (not shown). Moreover, in the absence of restimulation, BM cells produced very low levels of IFN $\gamma$ , granulocyte-macrophage colony-stimulating factor, tumor necrosis factor, IL-4, IL-5, IL-6, IL-10 and IL-17A (Supplementary figure 3c). Thus, MM development was associated with small variations in the availability of the ILC2-activating cytokines TSLP and IL-25 in the BM.

To determine the impact of MM-induced environmental changes on ILC2s, we analyzed the number and phenotype of BM ILC2s at different time points post-tumor cell inoculation. Overall, there was no significant difference in BM ILC2 numbers between naïve and MM-bearing mice even though a slight increase in ILC2 frequencies was observed at week 3 post-tumor cell inoculation (Figure 1a, b). Flow cytometry analyses of ILC2 markers revealed phenotypic alterations that correlated with tumor burden (Figure 1c–f). In the presence of MM, BM ILC2s expressed higher levels of the transcription factor GATA3, as well as CD117, KLRPG1 and CD25, whereas the expression of Sca1, CD127 and ICOS was decreased. By contrast, MM development did not affect the expression of the IL-33 receptor subunit ST2. To assess the effects of MM development on ILC2 function, we sorted ILC2s from naïve and MM-bearing mice and stimulated them *in vitro* with IL-2 and IL-33. Interestingly, IL-5, IL-6 and IL-13 production from ILC2s isolated from MM-bearing mice was slightly reduced (Supplementary figure 4), suggesting that MM development may drive ILC2 dysfunction. Collectively, these data establish that MM development is associated with phenotypic and functional alterations of BM ILC2s.

### Reconstitution of *Il2rg*<sup>-/-</sup> *Rag2*<sup>-/-</sup> mice with BM ILC2s has no effect on myeloma progression

To determine whether the presence of ILC2s influences myeloma growth, we used *Il2rg*<sup>-/-</sup> *Rag2*<sup>-/-</sup> mice that lack ILCs. We purified ILC2s from the BM of female *Id2*<sup>GFP/GFP</sup> mice and transferred them into *Il2rg*<sup>-/-</sup> *Rag2*<sup>-/-</sup> mice. We found that transferred BM ILC2s gave rise to a population of KLRG1<sup>hi</sup> ILC2s that preferentially accumulates in the spleen and liver (Figure 2a and Supplementary figure 5). *Il2rg*<sup>-/-</sup> *Rag2*<sup>-/-</sup> mice were injected with  $1 \times 10^4$  BM ILC2s and challenged 2 days later with Vk12653 MM cells. Analysis was performed 4 weeks after tumor cell inoculation. We detected low levels of IL-5 in the sera of ILC2-reconstituted *Il2rg*<sup>-/-</sup> *Rag2*<sup>-/-</sup> mice, whereas this cytokine was undetectable in control *Il2rg*<sup>-/-</sup> *Rag2*<sup>-/-</sup> mice (Figure 2b). This observation supports the predicted functional capacity of transferred BM ILC2s in *Il2rg*<sup>-/-</sup> *Rag2*<sup>-/-</sup> mice. However, control and ILC2-reconstituted *Il2rg*<sup>-/-</sup> *Rag2*<sup>-/-</sup> mice exhibited similar levels of serum IL-6 and IFN $\gamma$ . We failed to detect any IL-4 or IL-13 (data not shown). In agreement with the reported role of ILC2s in promoting eosinophil recruitment and proliferation,<sup>11,39</sup> we observed increased percentages and numbers of eosinophils in the BM, spleen and liver of ILC2-reconstituted *Il2rg*<sup>-/-</sup> *Rag2*<sup>-/-</sup> mice (Figure 2c, d). By contrast, control and ILC2-reconstituted *Il2rg*<sup>-/-</sup> *Rag2*<sup>-/-</sup> mice presented similar percentages of CD11b<sup>+</sup> myeloid cells, with no difference in major histocompatibility complex class II or CD206 expression (Figure 2c and data not shown). Interestingly, we observed a correlation between the percentages of ILC2s and eosinophils in the spleen and liver, but not in the BM (Figure 2e). Finally, malignant plasma cells were analyzed by flow cytometry in the different organs of control and ILC2-reconstituted *Il2rg*<sup>-/-</sup> *Rag2*<sup>-/-</sup> mice. Myeloma burden was similar in the presence or absence of ILC2s (Figure 2f, g). Of note, reconstitution of *Il2rg*<sup>-/-</sup> *Rag2*<sup>-/-</sup> mice with higher numbers of BM ILC2s ( $2.3 \times 10^4$  cells total, administered in three separate injections) similarly expanded eosinophils with no significant effect on MM growth (data not shown). Together, these data indicate that KLRG1<sup>hi</sup> ILC2s generated from the homeostatic proliferation of BM ILC2s mediate eosinophil expansion. However, neither KLRG1<sup>hi</sup> ILC2s nor increased eosinophil numbers significantly affected myeloma growth in *Il2rg*<sup>-/-</sup> *Rag2*<sup>-/-</sup> mice.

### Systemic treatment with IL-33 induces a population of circulating KLRG1<sup>hi</sup> ILC2s that preferentially accumulates in the spleen and liver

To characterize ILC2s' response to systemic treatment with IL-33, female wild-type (WT) mice were administered

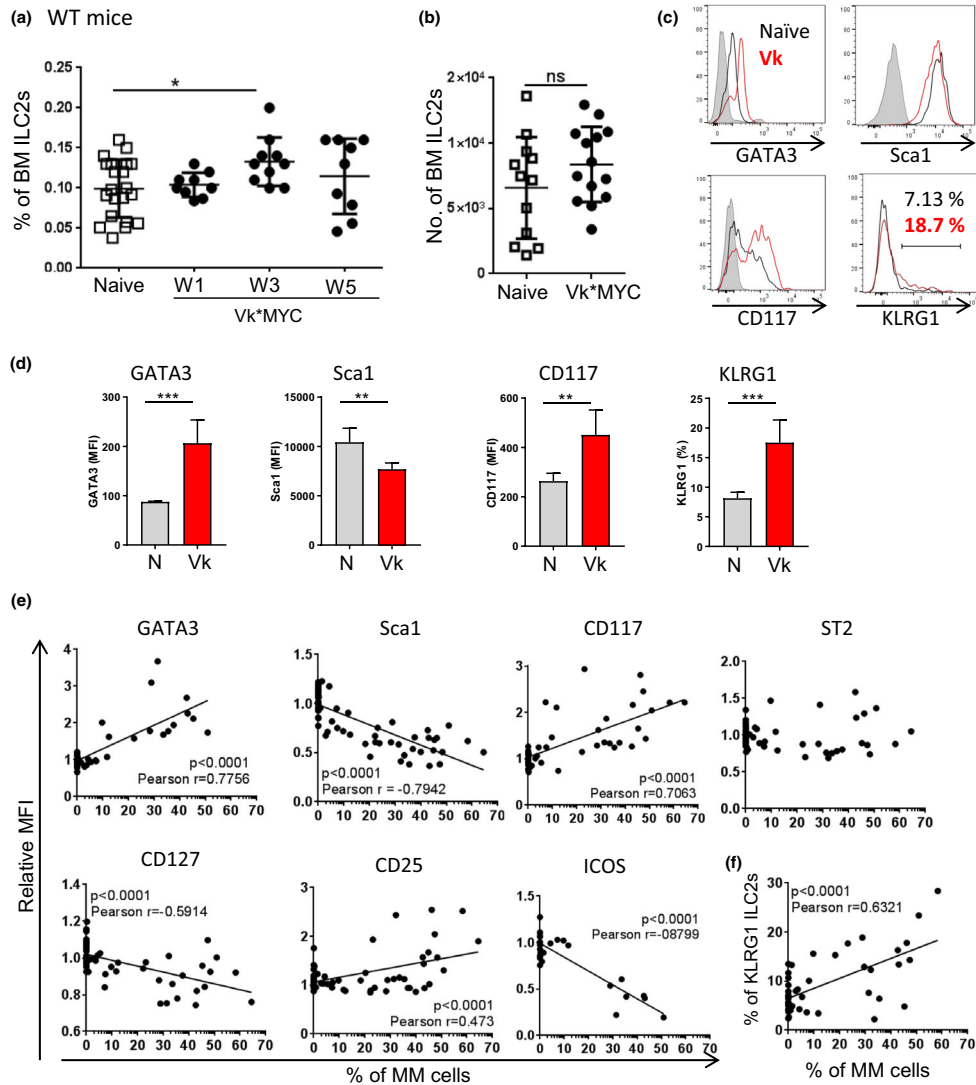


**Figure 1.** MM development is associated with phenotypic and functional alterations of BM ILC2s. **(a, b)** Female C57BL/6 WT mice were challenged intravenously (iv) with  $2 \times 10^6$  Vk12653 MM cells. Naïve age-matched female C57BL/6 WT mice were used as control. **(a)** At weeks 1, 3 and 5 post-tumor cell inoculation, ILC2 percentages within total BM CD45.2<sup>+</sup> cells were analyzed. Data were pooled from two independent experiments with 2 or 5 mice per group each and analyzed with a one-way ANOVA followed by Holm–Šidák multiple comparison test. \*  $P < 0.05$ . **(b)** Numbers of ILC2s per femur were determined at week 3 post-tumor cell inoculation. Data were pooled from three independent experiments with 2 or 5 mice per group each and analyzed with a Mann–Whitney  $U$ -test. **(c–f)** Male or female C57BL/6 WT or *Id2*<sup>GFP/</sup> mice were challenged iv with  $2 \times 10^6$  Vk12653 MM cells. Naïve sex- and age-matched mice were used as control. Marker expression on BM ILC2s was analyzed by flow cytometry at different times after Vk12653 cell inoculation. **(c)** Representative staining for GATA3, Sca-1, CD117 and KLRG1 on BM ILC2s from female C57BL/6 WT mice at week 5 post-tumor cell inoculation (red line). Staining in control naïve female C57BL/6 WT mice is shown in black and filled histograms represent the FMO. **(d)** Quantification of data shown in **c**. Data are shown as mean  $\pm$  s.d. of  $n = 5$  mice per group from one experiment, representative of two independent experiments. Data were analyzed with an unpaired  $t$ -test. \*\* $P < 0.01$ ; \*\*\* $P < 0.001$ . **(e)** The MFI of each marker in MM-bearing mice was normalized to the mean MFI obtained in control naïve mice. Graphs show correlation between the relative MFI of each marker and the percentages of malignant CD155<sup>+</sup> plasma cells (MM cells) in the BM. **(f)** Correlation between the percentages of KLRG1<sup>+</sup> ILC2s and MM cells in the BM of female mice. Data were pooled from two or seven experiments with a total of  $n = 28$  or 63 mice and analyzed with a Pearson correlation test. BM, bone marrow; FMO, fluorescence minus one; ILC2, Type 2 innate lymphoid cell; MFI, mean fluorescence intensity; MM, multiple myeloma; N, naïve; ns, not significant; Vk, challenged with Vk12653 MM cells; WT, wild type.

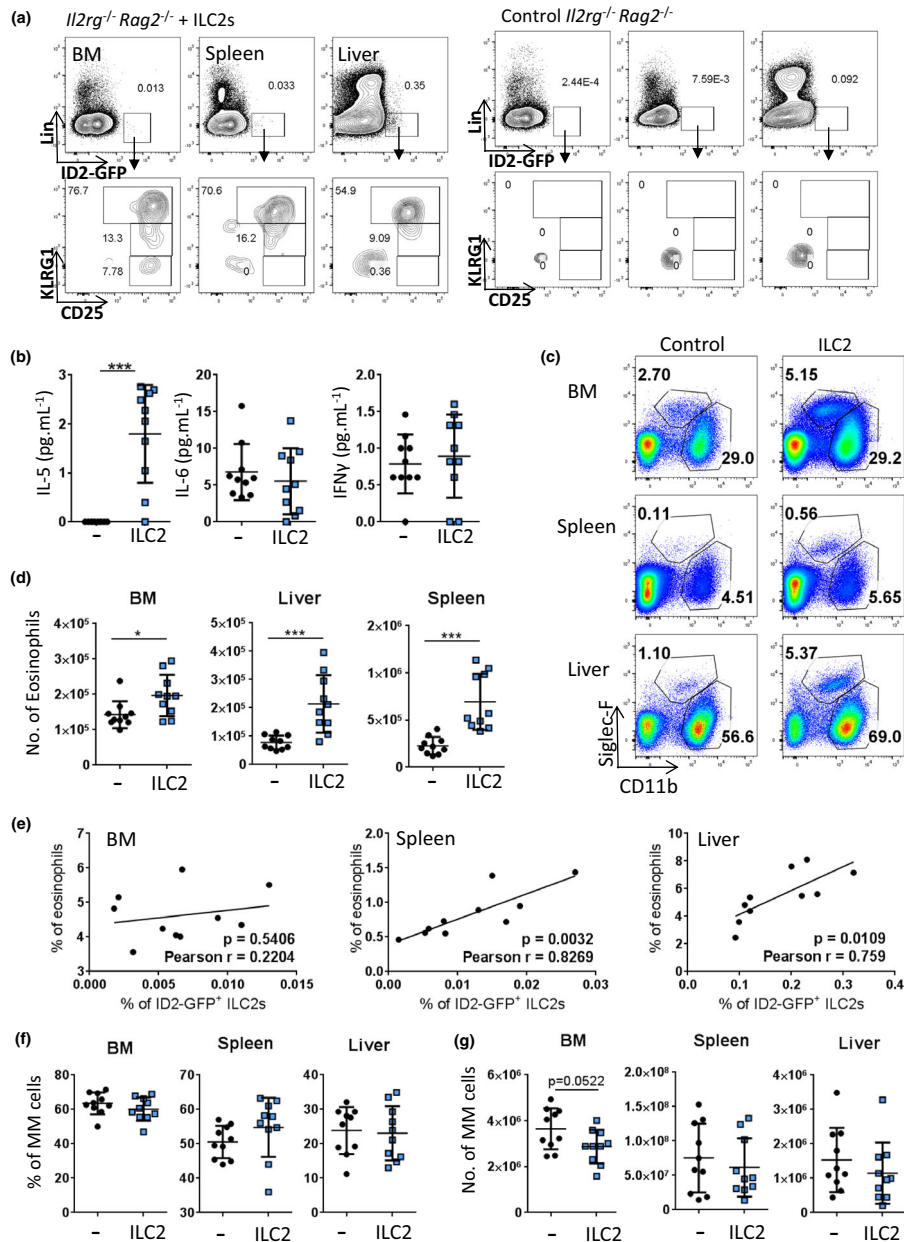


**Figure 2.** KLRG1<sup>hi</sup> ILCs promote eosinophil accumulation in MM-bearing mice but do not influence tumor burden. ILC2s were sorted from the BM of *Id2*<sup>GFP/GFP</sup> mice and injected intravenously (iv) into *Il2rg*<sup>-/-</sup> *Rag2*<sup>-/-</sup> mice (10 000 ILC2s per mouse). Two days later, ILC2-constituted *Il2rg*<sup>-/-</sup> *Rag2*<sup>-/-</sup> mice as well as control *Il2rg*<sup>-/-</sup> *Rag2*<sup>-/-</sup> mice were injected iv with 2 × 10<sup>6</sup> Vk12653 MM cells and analysis was performed on day 26 post-MM cell inoculation. **(a)** Cells are gated on live CD45.2<sup>+</sup> cells. The lineage cocktail used was TCR $\beta$ , TCR $\gamma\delta$ , CD3, CD5, CD19, CD11c. The percentages of ID2<sup>+</sup> cells and CD25/KLRG1 expressing subsets are shown. **(b)** Levels of IL-5, IL-6 and IFN $\gamma$  in the sera of control (-) and ILC2-reconstituted *Il2rg*<sup>-/-</sup> *Rag2*<sup>-/-</sup> mice were determined by cytometric bead array. **(c)** Percentages of eosinophils (CD11b<sup>int</sup> SiglecF<sup>+</sup>) and CD11b<sup>hi</sup> myeloid cells were analyzed by flow cytometry. **(d)** Quantification of eosinophil numbers in the BM, spleen and liver of control and ILC2-reconstituted *Il2rg*<sup>-/-</sup> *Rag2*<sup>-/-</sup> mice. **(e)** Percentages of Lin<sup>+</sup>ID2<sup>+</sup>CD25<sup>+</sup> ILC2s correlate with eosinophil percentages in the spleen and the liver but not in the BM of ILC2-reconstituted *Il2rg*<sup>-/-</sup> *Rag2*<sup>-/-</sup> mice. **(f)** Percentages and **(g)** absolute numbers of malignant CD155<sup>+</sup> plasma cells (MM cells) in the BM, spleen and liver of control or ILC2-reconstituted *Il2rg*<sup>-/-</sup> *Rag2*<sup>-/-</sup> mice were analyzed by flow cytometry. Data are from one experiment with *n* = 10 mice per group and were analyzed with a Mann-Whitney *U*-test (**b**, **d**, **f** and **g**) or with a Pearson correlation test (**e**). \**P* < 0.05; \*\*\**P* < 0.001. BM, bone marrow; IFN, interferon; IL, interleukin; ILC2, type 2 innate lymphoid cell; MM, multiple myeloma.

200 ng of IL-33 intraperitoneally on day 0 and day 2. ILC2s were analyzed on day 5 by flow cytometry. In the BM of IL-33-treated mice, we observed the emergence of a KLRG1<sup>hi</sup> ILC2 population resembling the one observed in ILC2-reconstituted-*Il2rg*<sup>-/-</sup> *Rag2*<sup>-/-</sup> mice (Figure 3a). Strikingly, KLRG1<sup>hi</sup> ILC2s were detected in every organ analyzed in mice receiving IL-33, including the spleen and inguinal lymph nodes that are normally devoid of KLRG1<sup>+</sup> ILC2s in naïve mice. In this analysis, we identified three populations of ILC2s: CD25<sup>+</sup>KLRG1<sup>-</sup>, CD25<sup>+</sup>KLRG1<sup>int</sup> and CD25<sup>low</sup>KLRG1<sup>hi</sup> ILC2s. Because CD25<sup>+</sup>KLRG1<sup>-</sup> ILC2s dominated in the BM of naïve female mice, we think that these cells might represent immature ILC2s and/or ILC2 progenitors. By contrast, CD25<sup>+</sup>KLRG1<sup>int</sup> cells were mostly found in the lung and mesenteric lymph nodes of naïve mice and we hypothesize that they are mature ILC2s. Finally, CD25<sup>low</sup>KLRG1<sup>hi</sup> ILC2s were found in every organ following IL-33 injections and we propose to call them inflammatory ILC2s because they resemble the inflammatory ILC2 population described by Huang *et al.*<sup>18</sup> Analysis of the kinetics of induction of inflammatory CD25<sup>low</sup>KLRG1<sup>hi</sup> ILC2s showed that they were detectable 3 days after the second injection of IL-33 and accounted for the important increase in ILC2 numbers observed in the lung and spleen (Figure 3b). The ability of IL-33 treatment to induce KLRG1<sup>hi</sup> ILC2s was confirmed in two subsequent experiments using *Rag2*<sup>-/-</sup> mice (Figure 3c). Similar to our observations in ILC2-reconstituted *Il2rg*<sup>-/-</sup> *Rag2*<sup>-/-</sup> mice, high numbers of KLRG1<sup>hi</sup> ILC2s were observed in the liver of IL-33-injected *Rag2*<sup>-/-</sup> mice. KLRG1<sup>hi</sup> ILC2s were also detected in the blood of IL-33-injected *Rag2*<sup>-/-</sup> mice. These results suggest that a population of circulating KLRG1<sup>hi</sup> ILC2s emerges in response to IL-33 treatment and populates highly vascularized organs including the spleen and the liver.

#### IL-33-induced KLRG1<sup>hi</sup> ILC2s have no effect on myeloma progression

Next, we investigated the potential role of IL-33-mediated activation of ILC2s in MM. WT mice were challenged with Vk12653 MM cells and 2 weeks later, mice received two injections of 200 ng of IL-33 twodays apart. At day 6 post-treatment, ILC2s defined as Lin<sup>-</sup>CD127<sup>+</sup>ST2<sup>+</sup>Scal<sup>+</sup> or Lin<sup>-</sup>CD127<sup>+</sup>CD25<sup>+</sup>KLRG1<sup>hi</sup> cells were present in the blood of IL-33-treated mice, but they were no longer detectable after 10 days (Figure 4a, b). Mice were killed at 4 weeks postmyeloma injection (i.e. 2 weeks post-IL-33 treatment) and organs were analyzed by flow cytometry. In agreement with data obtained in nontumor-bearing mice, we observed KLRG1<sup>hi</sup> ILC2s in the BM, spleen and liver of IL-33-injected mice, but not in phosphate-buffered saline (PBS)-treated mice (Figure 4c, d). Eosinophil numbers were significantly increased in IL-33-treated mice

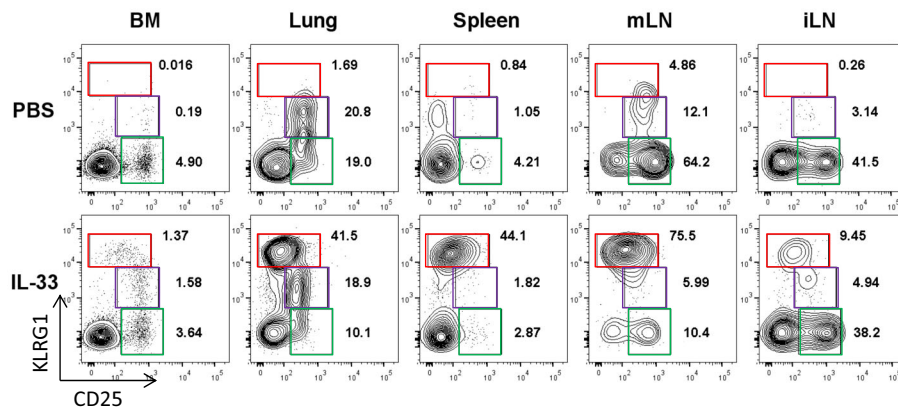
(Figure 4e). Yet, there was no difference in the percentages of CD11b<sup>+</sup> macrophages, nor in their expression of the M2-associated marker CD206 (data not shown). Moreover, there was no difference in myeloma burden between IL-33- and PBS-treated mice (Figure 4f). Similarly, IL-33 treatment had no effect on myeloma growth when started simultaneously with tumor injection, in either WT or *Rag2*<sup>-/-</sup> mice (not shown). Moreover, we did not detect any difference in survival following IL-33 treatment when WT, *Rag2*<sup>-/-</sup> or *Il2rg*<sup>-/-</sup> *Rag2*<sup>-/-</sup> mice were challenged with Vk12598, another Vk\*MYC myeloma cell line (Figure 4g). Thus, although a short course of IL-33 treatment induced the expansion of KLRG1<sup>hi</sup> ILC2s and increased eosinophil numbers, it had no influence on myeloma growth.

#### Combined administration of IL-33 with IL-12 and IL-18 induces a mixed type 1/type 2 response characterized by the production of IL-5, IL-13 and IFN $\gamma$

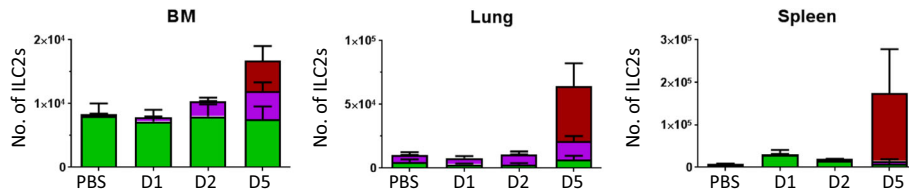
Given that IL-12 and IL-18 have previously been shown to promote the conversion of ILC2s into ILC1s,<sup>20</sup> and that IFN $\gamma$  secretion by ILC1s might limit tumor growth,<sup>4</sup> we investigated whether combined IL-12 and IL-18 administration could induce protective type 1 innate responses in our model. First, we observed that addition of IL-12 and IL-18 to our *in vitro* BM cultures induced IFN $\gamma$  production from BM ILC2s, suggesting that under these conditions, BM ILC2s acquired ILC1 functional properties (Figure 5a). However, stimulation with IL-12 and IL-18 did not alter ILC2 secretion of IL-5 and IL-13 (Supplementary figure 6). Of note, BM ILC2s from naïve and MM-bearing WT mice secreted similar amounts of IFN $\gamma$  upon stimulation with IL-2, IL-33, IL-12 and IL-18 (Supplementary figure 7).

Next, we investigated whether combination of IL-33 with IL-12 and IL-18 potentiates type 1 innate responses *in vivo*. First, *Rag2*<sup>-/-</sup> mice were injected with IL-33 on day 0, and with IL-33, with or without IL-12 and IL-18 (IL-12/IL-18), on day 2. Analysis of serum cytokine levels on day 4 revealed that mice that had received IL-33 alone developed a type 2 response characterized by increased levels of IL-5 and IL-13 (Figure 5b). Mice that additionally received IL-12/IL-18 exhibited a mixed type 2/type 1 response with increased levels of circulating IL-5, IL-13 and IFN $\gamma$ . On day 7, we observed increased percentages of NK1.1<sup>-</sup>CD127<sup>+</sup> non-NK ILCs in the blood of mice treated with IL-33, with no significant difference between mice treated with IL-33 only and IL-33 combined with IL-12/IL-18 (Figure 5c). Intracellular staining of NK1.1<sup>-</sup>CD127<sup>+</sup> cells indicated increased percentages of cells expressing the ILC2-associated transcription factor

(a) C57BL/6 WT mice



(b) WT C57BL/6 mice



(c) Rag<sup>-/-</sup> mice

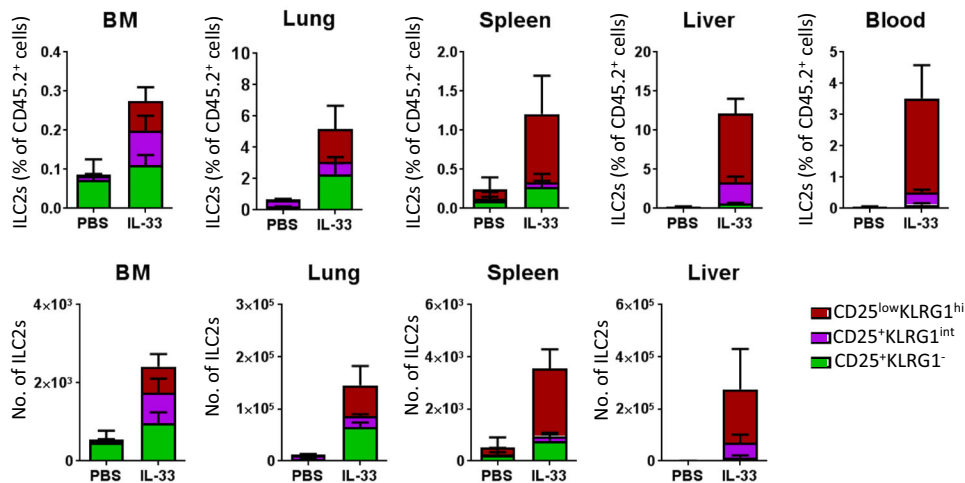


**Figure 3.** Systemic injection of IL-33 induces a population of circulating KLRG1<sup>hi</sup> ILC2s that accumulates in the liver. **(a, b)** Female C57BL/6 WT mice received two intraperitoneal (ip) injections of 200 ng of IL-33 on days 0 and 2. Groups of three mice were killed on day 1, day 2 (before the second injection of IL-33) and day 5; and ILC2s in the BM, lung, spleen, mLN and iLN were analyzed by flow cytometry. **(a)** Representative staining on day 5 after gating on live CD45.2<sup>+</sup>Lin<sup>-</sup>CD127<sup>+/low</sup> lymphocytes. The lineage cocktail used was Lin = TCRβ, TCRγδ, CD3, CD5, CD19, CD11c. Numbers indicate the percentages of CD25<sup>+</sup>KLRG1<sup>-</sup>, CD25<sup>+</sup>KLRG1<sup>int</sup> and CD25<sup>+</sup>KLRG1<sup>hi</sup> cells. **(b)** Quantification of CD25<sup>+</sup>KLRG1<sup>-</sup> (green), CD25<sup>+</sup>KLRG1<sup>int</sup> (purple) and CD25<sup>+</sup>KLRG1<sup>hi</sup> (red) ILC2 numbers in the BM, lung and spleen. Graphs show means ± s.d. from one experiment with *n* = 3 mice per group. **(c)** Female Rag2<sup>-/-</sup> mice received 2 ip injections of 200 ng of IL-33 on days 0 and 2 and CD25<sup>+</sup>KLRG1<sup>-</sup>, CD25<sup>+</sup>KLRG1<sup>int</sup> and CD25<sup>+</sup>KLRG1<sup>hi</sup> ILC2 subsets were analyzed by flow cytometry on day 5. Graphs show means ± s.d. of IL-33-injected (*n* = 3) and PBS-injected mice (*n* = 2). Data are from one experiment representative of two independent experiments. IFN, interferon; BM, bone marrow; IL, interleukin; ILC2, type 2 innate lymphoid cell; iLN, inguinal lymph nodes; mLN, mesenteric lymph nodes; PBS, phosphate-buffered saline; WT, wild type.

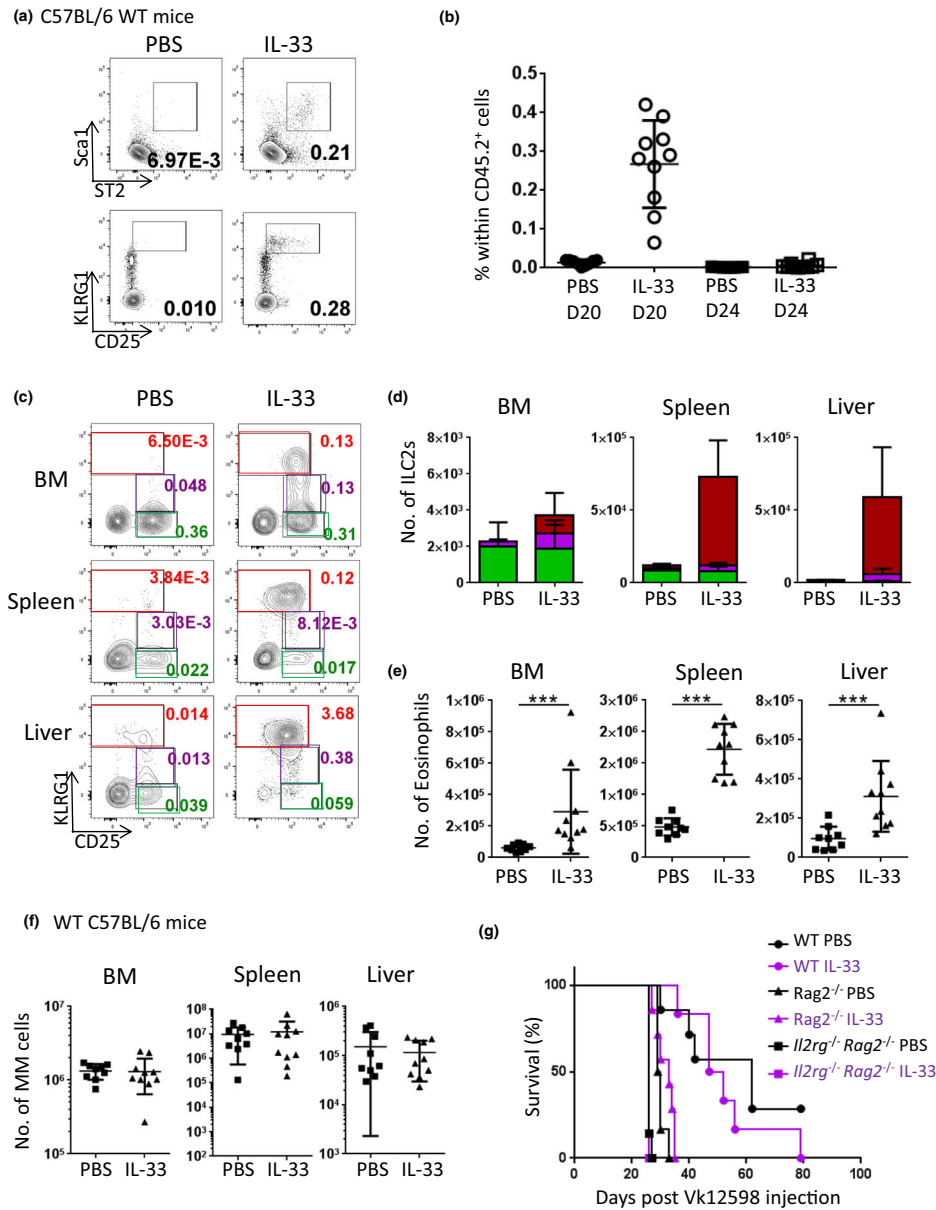


**Figure 4.** IL-33 treatment of myeloma-bearing mice expands KLRG1<sup>hi</sup> ILC2s but does not affect tumor growth. **(a–f)** Female C57BL/6 WT mice were injected intravenously (iv) with  $2 \times 10^5$  Vk12653 MM cells on day 0. Then, mice were injected intraperitoneally (ip) with 200 ng of recombinant IL-33 on days 14 and 16. **(a)** The presence of ILC2 in the blood was analyzed by flow cytometry on day 20. ILC2s were gated on CD45.2<sup>+</sup>Lin<sup>-</sup>CD127<sup>low/+</sup> cells as Sca1<sup>+</sup>ST2<sup>+</sup> (upper panel) or CD25<sup>+</sup>KLRG1<sup>hi</sup> (bottom panel). Numbers indicate the percentages of cells within live CD45.2<sup>+</sup> cells. The lineage cocktail used was TCR $\beta$ , TCR $\gamma\delta$ , CD11c, CD3, CD19. **(b)** Percentages of CD25<sup>+</sup>KLRG1<sup>hi</sup> ILCs were quantified in the blood on days 20 and 24 (i.e. 6 and 10 days, respectively, after the first injection of IL-33). **(c)** ILC2s were analyzed by flow cytometry on day 28 in the BM, spleen and liver. Representative dot plots gated on Lin<sup>-</sup>CD127<sup>low/+</sup> cells are shown. Numbers indicate the percentages of CD25<sup>+</sup>KLRG1<sup>int</sup>, CD25<sup>+</sup>KLRG1<sup>int</sup> and CD25<sup>+</sup>KLRG1<sup>hi</sup> cells within live CD45.2<sup>+</sup> cells. **(d)** Graphs show mean  $\pm$  s.d. of absolute numbers of CD25<sup>+</sup>KLRG1<sup>int</sup> (green), CD25<sup>+</sup>KLRG1<sup>int</sup> (purple) and CD25<sup>+</sup>KLRG1<sup>hi</sup> (red) ILCs as gated in **c**. **(e)** Numbers of eosinophils on day 28. **(f)** Numbers of CD155<sup>+</sup> malignant plasma cells (MM cells) on day 28. **(g)** C57BL/6 WT (circles), Rag2<sup>-/-</sup> (triangles) or Il2rg<sup>-/-</sup>Rag2<sup>-/-</sup> mice (squares) were injected intravenously (iv) with  $4 \times 10^5$  Vk12598 cells on day 0 and received two ip injections of 200 ng IL-33 (purple) or PBS (black) on days 0 and 2. Survival was monitored overtime. Data are from one experiment with **(a–f)**  $n = 10$  or **(g)**  $n = 7$  mice per group. **(e)** Data were analyzed with a Mann–Whitney  $U$ -test. \*\*\* $P < 0.001$ . BM, bone marrow; IL, interleukin; ILC2, type 2 innate lymphoid cell; MM, multiple myeloma; PBS, phosphate-buffered saline; WT, wild type.

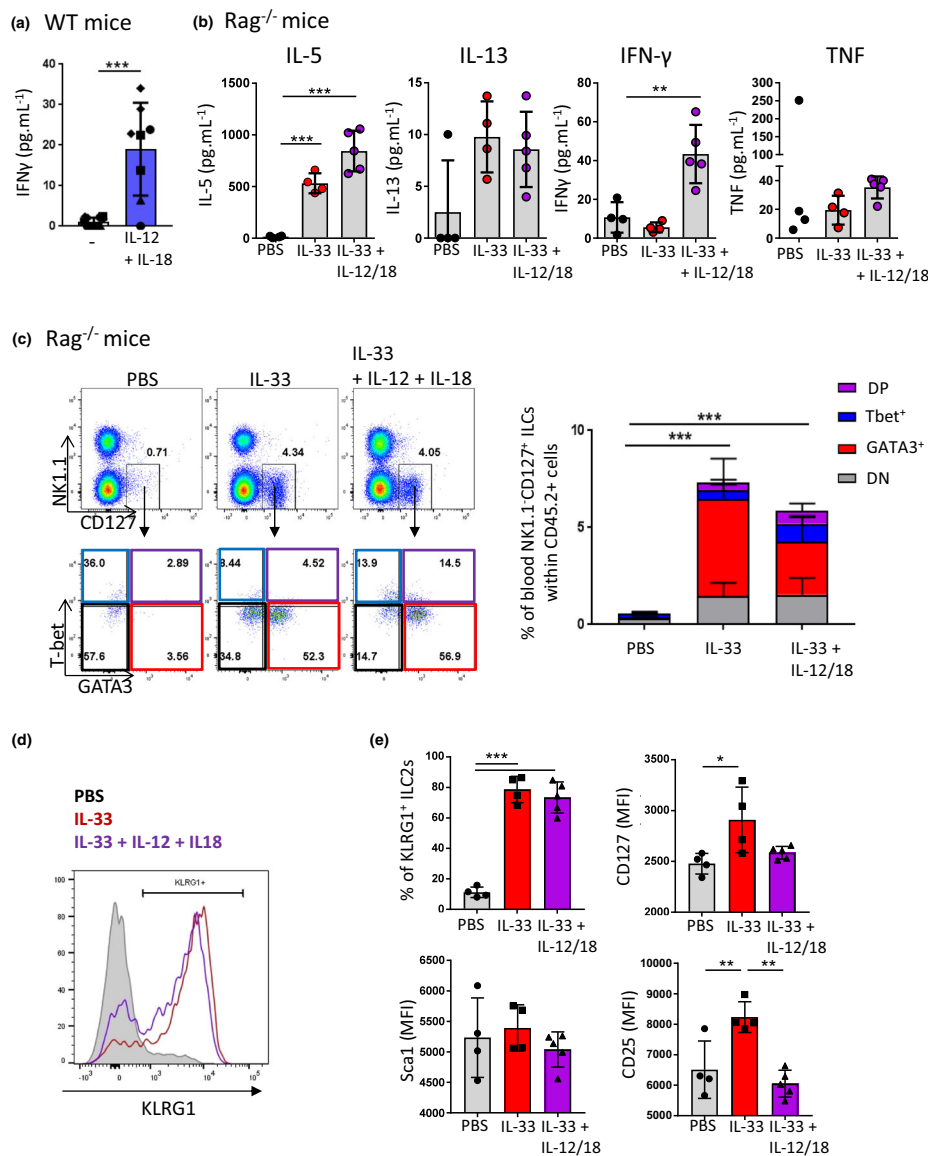


**Figure 5.** Combination of IL-33, IL-12 and IL-18 injections induces a mixed type 1/type 2 response in Rag $^{-/-}$  mice. **(a)** ILC2s were sorted from the BM of female *Id2*<sup>GFP/GFP</sup> mice and cultured overnight in the presence of IL-2 (40 ng mL $^{-1}$ ) and IL-33 (40 ng mL $^{-1}$ ) with or without IL-12 (1 ng mL $^{-1}$ ) and IL-18 (20 ng mL $^{-1}$ ). Cytokine levels in the culture supernatants were measured by CBA. Data are shown as mean  $\pm$  s.d. from four independent experiments. Data acquired within the same experiment are displayed with similar symbols; each symbol represents a technical replicate (culture well). Data were analyzed using a 2-way ANOVA with experiment and culture conditions as variables. **(b, c)** On day 0, female Rag2 $^{-/-}$  mice were injected with IL-33 [200 ng, intraperitoneal (ip)] or PBS as control. On day 2, mice were injected with IL-33, with or without IL-12 and IL-18 (200 ng, ip), or PBS as control. **(b)** Serum was collected on day 4 and cytokine levels were analyzed by CBA. **(c)** On day 7, blood was collected and ILCs were analyzed by flow cytometry. Cells were gated on live CD45.2 $^{+}$  lymphocytes and non-NK ILCs defined as NK1.1 $^{-}$ CD127 $^{+}$  were then divided into GATA3 $^{+}$ Tbet $^{-}$  (double negative: DN; black), GATA3 $^{+}$ Tbet $^{-}$  (red), GATA3 $^{+}$ Tbet $^{+}$  (blue) and GATA3 $^{+}$ Tbet $^{+}$  (DP: double positive; purple) ILCs. Numbers indicate the percentage of each population within the gate. **(d, e)** Marker expression on BM ILC2s (NK1.1 $^{-}$ CD127 $^{+}$ CD25 $^{+}$ Sca1 $^{+}$ ) was analyzed by flow cytometry on day 7. **(d)** Representative histogram showing KLRG1 expression on BM ILCs. Filled gray: PBS; red: IL-33; purple: IL-33 + IL-12 + IL-18. Data are from one experiment and are shown as representative FACS plots and mean  $\pm$  s.d. of four or five mice per group. Data were analyzed with **(b, e)** a one-way ANOVA followed by a Dunnett's multiple comparison *post hoc* test or **(c)** a two-way ANOVA followed by a Tukey's multiple comparison *post hoc* test. \*  $P < 0.05$ ; \*\*  $P < 0.01$ ; \*\*\*  $P < 0.001$ . BM, bone marrow; CBA, cytometric bead array; BM, bone marrow; FACS, flow cytometry staining; IL, interleukin; ILC2, type 2 innate lymphoid cell; MFI, mean fluorescence intensity; NK, natural killer; PBS, phosphate-buffered saline.

GATA3 in IL-33-treated mice, whereas the percentage of cells expressing the ILC1-associated transcription factor T-bet was increased in IL-33/IL-12/IL-18-treated mice (Figure 5c). Moreover, similar to IL-33 treatment, IL-33/IL-12/IL-18 treatment led to upregulation of KLRG1 on BM ILC2s (Figure 5d, e). Overall, these data indicate that a mixed type 1/type 2 response was induced with the IL-33/IL-12/IL-18 combination.

To determine whether increased number of IL-12/IL-18 injections improved type 1 responses, *Rag2*<sup>-/-</sup> mice were injected with IL-33 on days 0 and 2, and mice received daily injections of IL-12/IL-18 from day 4 to day 7 (Supplementary figure 8). However, four consecutive daily injections of IL-12/IL-18 failed to increase the percentages of T-bet<sup>+</sup> ILCs. Moreover, we noticed that, in this experiment, mice receiving IL-12/IL-18 had ruffled fur, suggesting that increased doses of IL-12/IL-18 may have been toxic. Therefore, we decided to only administer one injection of IL-12/IL-18 in subsequent experiments.

#### Administration of IL-12 and IL-18 protects *Rag*<sup>-/-</sup> mice against MM

To determine the effect of exogenous administration of IL-12/IL-18 on MM progression, *Rag1*<sup>-/-</sup> mice were challenged with Vk12653 MM cells and 4 days later, mice were injected with IL-12 and IL-18. This single injection of IL-12/IL-18 prolonged survival (Figure 6a). NK cells are known to be important mediators of type 1 responses.<sup>40</sup> Therefore, we used anti-asialoGM1 (anti-asGM1) antibodies (Abs) that are known successfully to deplete NK cells in the Vk\*MYC MM model.<sup>34,41</sup> Surprisingly, IL-12/IL-18 injection was still protective in anti-asGM1 Ab-treated mice. Flow cytometry analyses revealed that both NK cells and CD11b<sup>+</sup> myeloid cells produced IFN $\gamma$  following IL-12/IL-18 injection (Figure 6b, c). Moreover, we observed detectable levels of IFN $\gamma$  in the serum of *Il2rg*<sup>-/-</sup> *Rag2*<sup>-/-</sup> mice treated with IL-12/18, suggesting that this treatment induces type 1 innate response from myeloid cells (Supplementary figure 9). Together, these data demonstrate that exogenous administration of IL-12 and IL-18 protects mice against MM. Given that mice treated with anti-asGM1 Abs were still protected, we propose that the anti-myeloma effect was at least partially mediated by IL-12/IL-18-activated myeloid cells.

#### IL-33 favors type 2 innate responses and abolishes type 1 protection against MM

Finally, we wanted to determine the effect of the mixed type 1/type 2 response induced by IL-33/IL-12/IL-18 on MM progression. Female *Rag2*<sup>-/-</sup> mice were challenged

with Vk12653 MM cells and divided into three treatment groups: PBS control, IL-12/IL-18 and IL-33/IL-12/IL-18. Of note, an IL-33 only group was not included as we previously showed that IL-33 alone has no effect on MM growth (Figure 4f and g). IL-33 was administered on days 2 and 4, and IL-12/IL-18 on day 4 post-MM challenge. Cytokine analysis in the serum on day 5 confirmed a type 1 response in the IL-12/IL-18 group characterized by high levels of IFN $\gamma$  and tumor necrosis factor, whereas the type 2 cytokines IL-5 and IL-13 were increased in the IL-33/IL-12/IL-18-treated group (Supplementary figure 10a). We also detected low percentages of KLRG1<sup>hi</sup> CD127<sup>+</sup>NK1.1<sup>-</sup> ILCs in the blood of IL-33/IL-12/IL-18-treated mice but not in the two other groups (Supplementary figure 10b). On day 25, serum M-protein levels of IL-12/IL-18-treated mice were significantly decreased compared with PBS and IL-33/IL-12/IL-18-treated groups (Figure 7a). These data confirm the protection induced by a single injection of IL-12/IL-18 and indicate that IL-33 abolishes this protection. Survival analyses further confirmed that exogenous administration of IL-33 reverses the anti-MM effects of IL-12/IL-18 injection (Figure 7b). Similar data were obtained in another experiment performed with male *Rag1*<sup>-/-</sup> mice (Figure 7c). In a third experiment, female *Rag1*<sup>-/-</sup> mice were killed on day 30 post-MM challenge for flow cytometry analysis. Quantification of myeloma burden confirmed that the protection conferred by IL-12 and IL-18 was hampered by IL-33 treatment because myeloma cell numbers were significantly decreased in the liver of IL-12/IL-18- but not IL-33/IL-12/IL-18-treated mice (Figure 7d). Similarly, male mice treated with IL-12/IL-18 showed decreased myeloma burden in their BM, spleen and liver, but this protection was abolished in IL-33/IL-12/IL-18-treated mice (Figure 7e).

We found that, similar to single cytokine injections of IL-33, IL-33/IL-12/IL-18 treatment increased the percentage of BM ILC2s expressing KLRG1 in female *Rag1*<sup>-/-</sup> mice, whereas IL-12/IL-18 treatment had no effect on KLRG1 expression levels (Figure 8a). Consequently, we observed increased KLRG1<sup>hi</sup> ILC2s in the BM, spleen and liver of IL-33/IL-12/IL-18-treated female mice when compared with PBS- and IL-12/IL-18-treated mice (Figure 8b, c), as well as minor changes in NK1.1<sup>+</sup> cell numbers (Figure 8d). Increase in KLRG1<sup>hi</sup> ILC2s was also observed in the liver of IL-33/IL-12/IL-18-treated male mice (data not shown), thereby indicating that IL-33 had similar effect in both sexes. Finally, eosinophils were expanded in IL-33/IL-12/IL-18-treated mice when compared with PBS or IL-12/IL-18-treated mice (Figure 8e). Together, these results support the idea that, in both males and females, IL-33 induces type 2 responses that block protective type 1 immunity against MM.

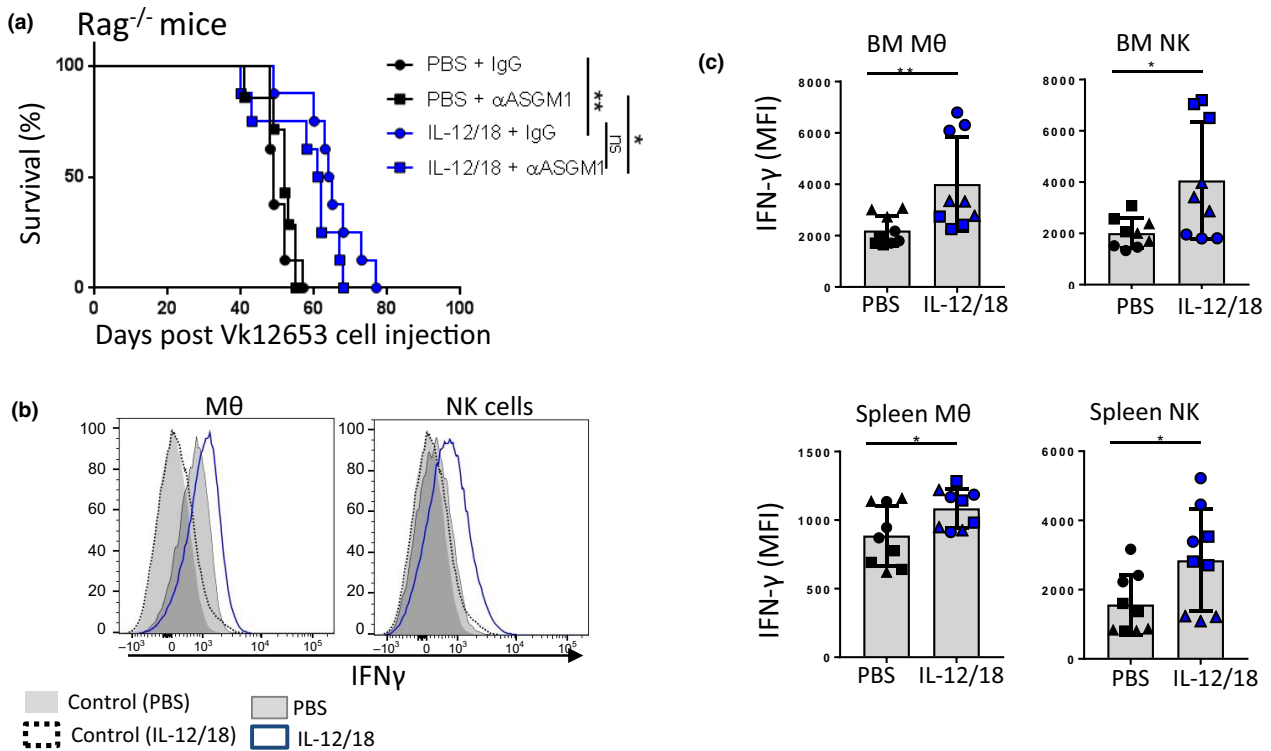


**Figure 6.** Administration of IL-12 and IL-18 induces IFN $\gamma$  production and prolongs the survival of MM-challenged Rag<sup>-/-</sup> mice. **(a)** Female Rag1<sup>-/-</sup> mice were challenged with VK12653 cells [ $2 \times 10^6$  cells, intravenously (iv)] on day 0. Mice were treated with anti-asialoGM1 (asGM1) Abs [100  $\mu$ g, intraperitoneal (ip)] on days 3, 7 and 11 or control IgG. Mice received a single injection of IL-12 and IL-18 (200 ng, ip) or PBS as control on day 7. Survival was analyzed using a log-rank test. Data are from one experiment with  $n = 7$  or 8 mice per group. **(b, c)** Rag2<sup>-/-</sup> mice received a single injection of IL-12 and IL-18 (200 ng, ip) or PBS as control. One day later, spleen and BM cells were collected and restimulated for 90 min in PMA–ionomycin plus transport inhibitors. IFN $\gamma$  production by CD11b<sup>+</sup> myeloid cells (M $\theta$ ) and NK1.1<sup>+</sup> NKp46<sup>+</sup> NK cells was determined by intracellular staining. **(b)** Representative staining. NK cells and M $\theta$  from PBS- (gray) and IL-12/IL-18- (blue) treated mice. CD11b<sup>-</sup>NK1.1<sup>-</sup> cells from these mice are shown as control (same control data are used for both graphs). **(c)** Data were pooled from three experiments, with a total of  $n = 9$  mice, and analyzed with a Mann–Whitney  $U$ -test. Data acquired within the same experiment are displayed with similar symbols. \* $P < 0.05$ ; \*\* $P < 0.01$ . BM, bone marrow; IFN, interferon; IL, interleukin; MM, multiple myeloma; PBS, phosphate-buffered saline; PMA, phorbol myristate acetate.

## DISCUSSION

There is conflicting information regarding the implication of ILC2s in cancer and the potential therapeutic activity of IL-33. In this study, we observed that ILC2s and a short duration of IL-33 treatment have no impact on MM progression, in the absence of additional therapy. However, we found that IL-33 antagonized the protective effect of IL-12/IL-18 cytokine therapy. Our data support the idea that systemic administration of IL-33 induces a population of circulating KLRG1<sup>hi</sup> ILC2s that inhibits protective type 1 immune responses against MM.

The role of ILC2s in cancer is unclear. ILC2s have alternatively been defined as protective or pathologic in various mouse and human cancer studies.<sup>4,5</sup> In this report, using ILC2-reconstituted *Il2rg*<sup>-/-</sup> Rag2<sup>-/-</sup> mice and IL-33-mediated expansion of ILC2s, we discard a major role of

ILC2s in regulating MM development and growth. Our results contrast with previous studies showing a protective role of IL-33-activated ILC2s against mouse subcutaneous tumors and metastases.<sup>9,10</sup> Apart from the localization of the tumor (BM, spleen and liver *versus* subcutaneous), an important difference between these studies and ours is the mode of IL-33 delivery. Here, we used a short systemic IL-33 treatment (two intravenous injections over 5 days), whereas other studies utilized IL-33-secreting tumors.<sup>9,10</sup> While our treatment was sufficient to expand ILC2s in any organ analyzed, it may not have been sufficient to sustain ILC2 activation. This might explain why chronic exposure of tumor-infiltrating ILC2s to IL-33 could protect against cancer,<sup>9,10</sup> whereas systemic bolus injections of IL-33 used in this study were ineffective.

Very few studies have analyzed ILC2s in the context of hematological cancers. Increased percentages of circulating

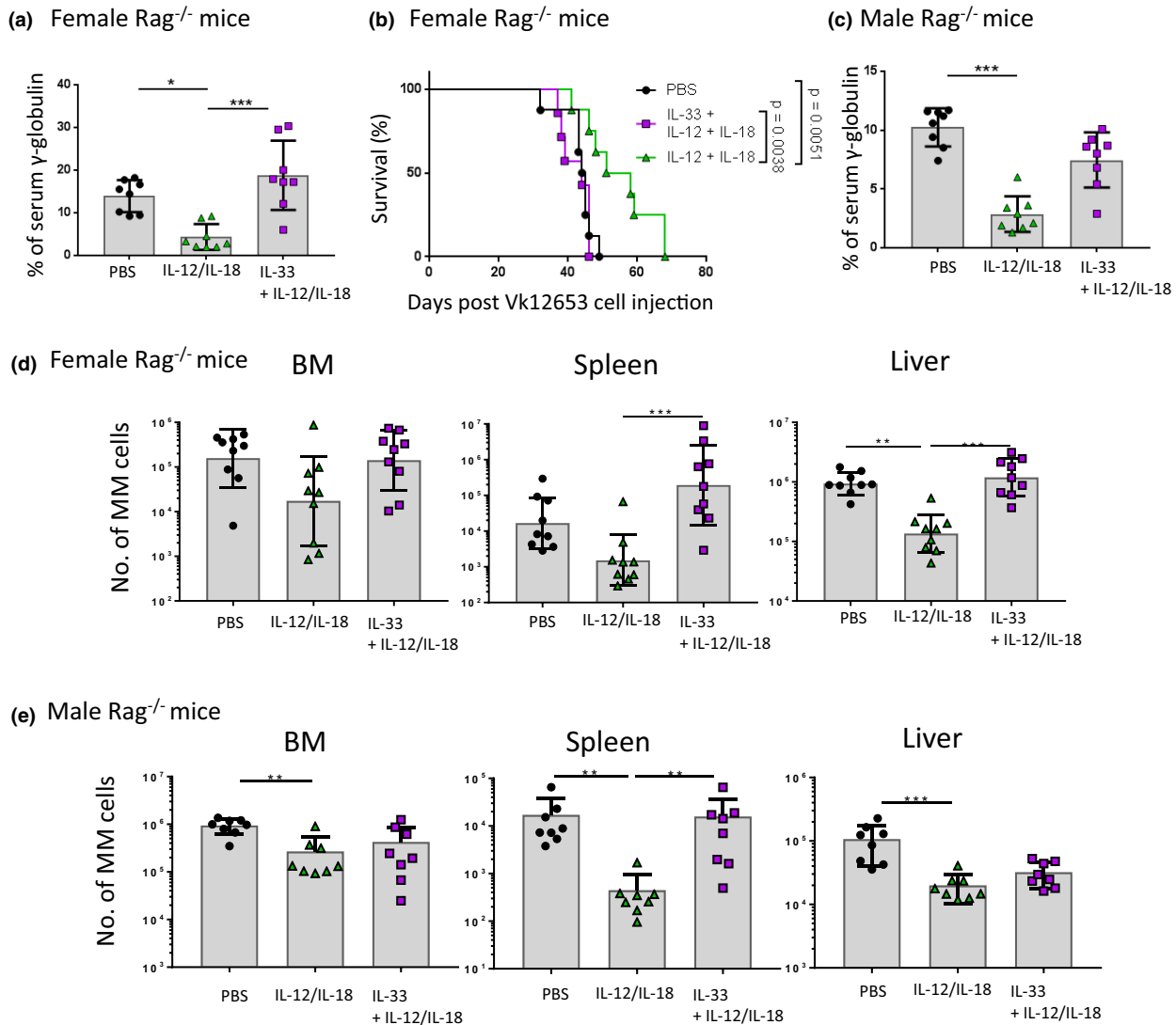


**Figure 7.** Exogenous administration of IL-33 abolishes the anti-myeloma effect of IL-12 and IL-18. Female Rag2<sup>-/-</sup> mice (**a, b**), male Rag1<sup>-/-</sup> mice (**c, e**) and female Rag1<sup>-/-</sup> mice (**d**) were challenged with Vk12653 MM cells [ $2 \times 10^6$  cells, intravenously (iv)] on day 0. Mice received injections of IL-33 [200 ng, intraperitoneal (ip)] or PBS as control on days 2 and 4. Some mice also received IL-12 and IL-18 (200 ng, ip) on day 4. (**a, c**) M-protein levels were analyzed by serum electrophoresis on day 23 (**c**) or day 25 (**a**). Data are shown as mean  $\pm$  s.d. of one experiment with  $n = 8$  mice per group and were analyzed with a Kruskal–Wallis test followed by Dunn’s multiple comparison *post hoc* test. (**b**) Survival was monitored overtime. Data were analyzed with a log-rank test. (**d, e**) Mice were killed on day 30 for flow cytometry analysis. Number of myeloma cells in the BM, spleen and liver were quantified. Data are shown as geometric mean  $\pm$  s.d. of one experiment with  $n = 8$  or 9 mice per group and were analyzed with a Kruskal–Wallis test followed by Dunn’s multiple comparison *post hoc* test. \*  $P < 0.05$ ; \*\*  $P < 0.01$ ; \*\*\*  $P < 0.001$ . BM, bone marrow; IL, interleukin; MM, multiple myeloma; PBS, phosphate-buffered saline.

ILC2s were observed in patients diagnosed with acute promyelocytic leukemia,<sup>42</sup> but not in the other acute myeloid leukemia subtypes.<sup>43</sup> Here, we showed comparable ILC2 numbers in the BM of naïve and MM-challenged mice. Interestingly, BM ILC2s from MM-challenged mice expressed increased levels of GATA3, CD117, CD25 and KLRG1, and decreased levels of Sca1 and CD117. These phenotypic changes might indicate a progressive maturation

of BM ILC2s in the presence of myeloma. Moreover, we found that MM growth is associated with decreased ability of BM ILC2s to produce cytokines when stimulated with IL-2 and IL-33. Although ILC2s do not seem to influence the growth and dissemination of myeloma cells, functional alterations of ILC2s might have important implications for the resolution of infections that constitute a major cause of morbidity and mortality for MM patients.<sup>44,45</sup>

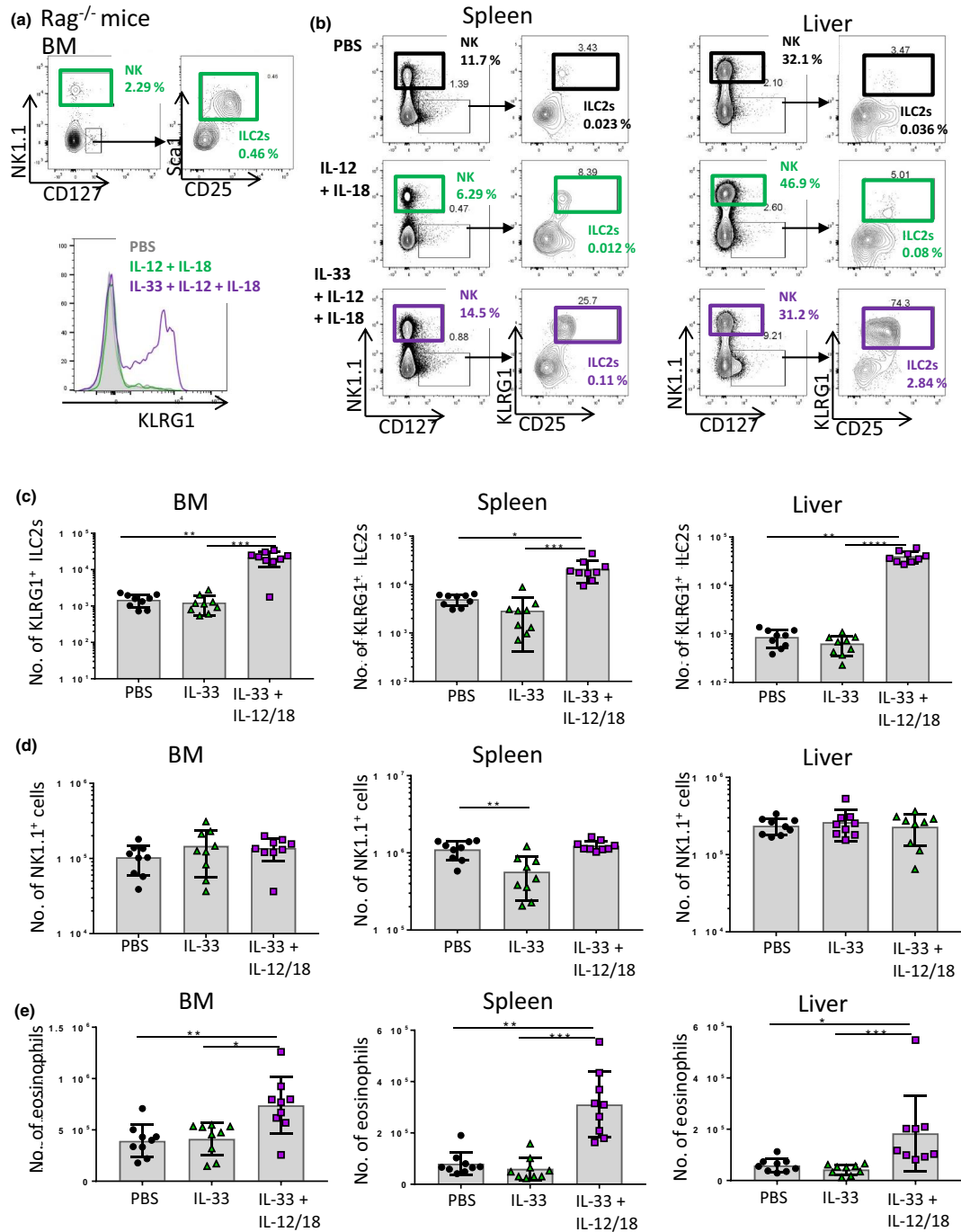


**Figure 8.** ILC2s and eosinophils are expanded in IL-33/IL-12/IL-18-treated mice but not in mice receiving IL-12/IL-18 only. Female Rag1<sup>-/-</sup> were challenged with Vk12653 MM cells [ $2 \times 10^6$  cells, intravenously (iv)] on day 0. Mice received injections of IL-33 [200 ng, intraperitoneal (ip)] or PBS as control on days 2 and 4. Some mice also received IL-12 and IL-18 (200 ng, ip) on day 4. Mice were killed on day 30 for flow cytometry analysis. **(a)** BM ILC2s (gated as NK1.1<sup>+</sup>CD127<sup>+</sup>CD25<sup>+</sup>Sca1<sup>+</sup>) were analyzed for their expression of KLRG1. Gray: PBS; green: IL-12 + IL-18; purple: IL-33 + IL-12 + IL-18. **(b)** Representative dot plot graphs showing the percentages of NK cells and KLRG1<sup>hi</sup> ILC2s in the liver and spleen. Cells were gated on CD45.2<sup>+</sup> live lymphocytes. **(c)** Absolute numbers of KLRG1<sup>hi</sup> ILC2s. **(d)** Absolute numbers of NK cells/ILC1s (gated as CD127<sup>+</sup>NK1.1<sup>+</sup>). **(e)** Absolute numbers of eosinophils (Siglec-F<sup>+</sup>). Data are shown as geometric mean  $\pm$  s.d. of one experiment with  $n = 9$  mice per group and were analyzed with a Kruskal–Wallis test followed by Dunn’s multiple comparison *post hoc* test. BM, bone marrow; IL, interleukin; ILC2, type 2 innate lymphoid cell; MM, multiple myeloma; NK, natural killer; PBS, phosphate-buffered saline.

The mechanisms responsible for altering ILC2 phenotype and function during the course of MM disease remain unknown. In the myeloma-infiltrated BM, hypoxia and sustained inflammation associated with the establishment of an immunosuppressive milieu are likely to influence ILC2 responses.<sup>46</sup> ILC2s may interact with other immune cells or with stromal cells, either through cell-to-cell contact or through the release of soluble factors. We screened different cytokines and observed a slight increase in the ILC2-activating cytokine TSLP in myeloma-infiltrated BM, suggesting that TSLP might contribute to the phenotypic changes of ILC2s observed in the presence of MM. Moreover, ILC2s express the immune checkpoint PD-1 whose ligand, PD-L1, is highly expressed in the myeloma microenvironment.<sup>47,48</sup> Therefore, PD-1/PD-L1 interactions might drive ILC2 exhaustion in MM.

The leading paradigm that ILCs are tissue-resident cells that arise from early progenitors seeding the organs during the embryonic stage has recently been challenged with the description of inflammatory ILC2s emerging in the blood in response to IL-25.<sup>49,50</sup> Supporting the hypothesis of migratory ILC2s, a cell population displaying the phenotypic and functional properties of tissue-resident ILC2s can be detected in the human blood.<sup>51</sup> We found that ILC2s circulate in the blood a few days after the injection of IL-33. Our data strongly support the idea that, upon activation, ILC2s lose their tissue-residency properties and enter the bloodstream. The progeny link between the different populations of tissue-resident and migratory ILC2s remains unclear. Huang *et al.* described a population of ST2<sup>+</sup>KLRG1<sup>hi</sup> inflammatory ILC2s that arise from gut-resident ILC2s following IL-25 stimulation or helminth infection; these inflammatory ILC2s enter the bloodstream and circulate to the lung where they regenerate the pool of “natural ILC2s”.<sup>50</sup> While systemic treatment with IL-33 has been shown to expand KLRG1<sup>hi</sup> ILC2s in mouse mesenteric lymph nodes or liver,<sup>19,52</sup> it is currently unclear whether all described inflammatory KLRG1<sup>hi</sup> ILC2s constitute a single population with a common origin, or whether different subsets arise in different organs and in response to different stimulations. Notably, inflammatory ILC2s described in this study differ from IL-25/helminth-induced inflammatory ILC2s by their high expression of the IL-33 receptor subunit ST-2.<sup>18,19</sup> This observation suggests the existence of different subsets of KLRG1<sup>hi</sup> inflammatory ILC2s.

Several pieces of evidence indicate that, unlike IL-25/helminth-induced ILC2s,<sup>50</sup> IL-33-induced KLRG1<sup>hi</sup> ILC2s observed in this study are derived from the BM. First, CD25<sup>+</sup>KLRG1<sup>int</sup> ILC2s were increased in the BM early after the first injection of IL-33, indicating a possible maturation pathway from CD25<sup>+</sup>KLRG1<sup>-</sup> ILC2 precursors

to CD25<sup>+</sup>KLRG1<sup>int</sup> ILC2s that might finally differentiate into CD25<sup>low</sup>KLRG1<sup>hi</sup> ILC2s in proinflammatory conditions. Moreover, we observed a similar population of KLRG1<sup>hi</sup> ILC2s in highly vascularized organs (spleen and liver) of *Il2rg*<sup>-/-</sup> *Rag2*<sup>-/-</sup> mice injected with BM ILC2s. Finally, our data are in agreement with a previous study indicating that IL-33 promotes ILC2 egress from the BM.<sup>53</sup> However, it is possible that several populations of KLRG1<sup>hi</sup> ILC2s with diverse origins coexist in our model. Notably, the hypothesis that IL-33-induced lung CD25<sup>low</sup>KLRG1<sup>hi</sup> ILC2s are derived from lung-resident CD25<sup>+</sup>KLRG1<sup>int</sup> ILC2s would be in agreement with data from Schneider *et al.* showing that helminth infection expands local ILC2 pools at the site of inflammation.<sup>54</sup> A limitation of our study is the lack of analysis of ILC2s in the intestine. However, IL-25 is likely to play a more important role than IL-33 on the regulation gut-resident ILC2s.<sup>14</sup> Considered in the context of the current literature, our results indicate the existence of two distinct inflammatory KLRG1<sup>hi</sup> ILC2s: ST2<sup>-</sup> IL-25-induced ILC2s that are derived from gut ILC2s and traffic to the lung,<sup>18,50</sup> and ST2<sup>+</sup> IL-33-induced ILC2s described here that are likely to emerge from the BM and preferentially populate the spleen and liver.

Our data showing accumulation of ILC2s in the liver of ILC2-reconstituted *Il2rg*<sup>-/-</sup> *Rag2*<sup>-/-</sup> mice contrast with a previous study which did not report ILC2s in the liver following the injection of Lin<sup>-</sup>Scal<sup>+</sup>CD25<sup>+</sup>Id2<sup>hi</sup> BM ILC2s to *Il2rg*<sup>-/-</sup> *Rag2*<sup>-/-</sup> mice.<sup>32</sup> While the reasons for this discrepancy remain unclear, we should note two factors that might have influenced the outcome of these experiments: the background of host *Il2rg*<sup>-/-</sup> *Rag2*<sup>-/-</sup> mice (BALB/c in the study by Hoyler *et al.*<sup>32</sup> and C57BL/6 in this study) and the mouse microbiota that is likely to differ between facilities. The idea that ILC2 migration is microbial mediated is an appealing hypothesis.<sup>55</sup> In this context, differences in microbiota might influence the circulating properties of ILC2s and thereby their accumulation in the liver. In agreement with our data, other studies reported expansion of liver ILC2s following systemic administration or hepatic expression of IL-33.<sup>52,56,57</sup> Moreover, in a recent review, Martinez-Gonzalez *et al.* indicated that they observed increased ILC2 numbers in the blood and liver a few weeks after activation, although they did not specify the type of activation.<sup>58</sup> In light of these findings, we propose that systemic administration of IL-33 induces a population of blood-circulating ILC2s that preferentially expand in the liver.

Our data confirm the existence of sex-driven differences in ILC2 biology.<sup>35,37,38</sup> Interestingly, compared with women, men are slightly more likely to develop MM. However, given the minor role played by ILC2 in MM pathology, sex-driven differences in ILC2s are

unlikely to underpin sex-driven differences in susceptibility to MM. Importantly, while most experiments of this study were performed in female mice, we have found that IL-12/IL-18 treatment protects both male and female mice against MM, and that additional injection of IL-33 reverses this protection and induces KLRG1<sup>hi</sup> ILC2s in both sexes.

We established that a single injection of IL-12/IL-18 was sufficient to delay myeloma progression in Rag-deficient mice. These results are consistent with the ability of these cytokines to induce a type 1 immune response characterized by the production of IFN $\gamma$  and the protective role of IFN $\gamma$  in cancer.<sup>59</sup> NK cells are known to be potent producers of IFN $\gamma$  in response to IL-12 and IL-18.<sup>40</sup> Surprisingly, we found that anti-asGM1 Ab treatment (known to deplete NK cells) did not significantly affect IL-12/IL-18-mediated protection against MM, although we observed a nonsignificant trend toward decreased survival when NK cells were depleted during IL-12/18 injection. Moreover, we found that IL-12/18 treatment induced systemic IFN $\gamma$  response in *Il2rg*<sup>-/-</sup> *Rag2*<sup>-/-</sup> mice, indicating that a type 1 response could be mounted even in the absence of NK cells. However, in agreement with NK cell role in sustaining type 1 responses, increased levels of IFN $\gamma$  were observed in *Il2rg*<sup>-/-</sup> *Rag2*<sup>-/-</sup> mice that had received NK cell transfer. Flow cytometry analysis confirmed that both NK cells and CD11b<sup>+</sup> myeloid cells produce IFN $\gamma$  in response to IL-12/18. While additional experiments will be required to definitively rule out a role of NK cells, our data suggest that macrophages, which are also endowed with anti-tumor properties and respond to IL-12 and IL-18,<sup>60,61</sup> might protect against MM in our model.

We decided to investigate the potential synergy between IL-33 and IL-12/IL-18 treatments for two reasons: (i) published studies suggested that IL-33 together with IL-12 promotes type 1 immunity,<sup>62,63</sup> and (ii) we hypothesized that IL-12/IL-18 might promote the differentiation of IL-33-expanded ILC2s into IFN $\gamma$ -secreting ILC1s.<sup>20</sup> However, we were not able to induce ILC2–ILC1 differentiation *in vivo* and we found that IL-33 treatment abolishes the therapeutic effect of IL-12/IL-18 administration. Loss of protection in IL-33/IL-12/IL-18-treated mice was associated with increased circulating levels of IL-5 and IL-13 and decreased levels of IFN $\gamma$  and tumor necrosis factor. These findings indicate that IL-33 induces a type 2 innate immune response that inhibits anti-myeloma type 1 innate immunity.

The precise mechanisms by which IL-33 counteracts the therapeutic effect of IL-12/IL-18 are not fully elucidated. We hypothesized that IL-12/IL-18 might induce M1 polarization of macrophages that would contribute to

tumor clearance, whereas type 2 cytokines produced by IL-33-induced ILC2s might promote M2 macrophages. However, flow-cytometric analysis of myeloid populations in cytokine-treated mice did not reveal drastic modifications of M1/M2 polarization, at least in terms of CD206 and major histocompatibility complex class II expression. An outstanding question is the importance of ILC2s for IL-33-mediated inhibition of IL-12/IL-18 therapeutic efficacy, for IL-33 might directly act on myeloid cells in an ILC2-independent manner.

In conclusion, our study describes a population of blood-circulating inflammatory KLRG1<sup>hi</sup> ILC2s that responds to IL-33 and establishes a negative role of IL-33 in the regulation of protective type 1 innate immunity against MM. Our data indicate that IL-12 and IL-18, but not IL-33, should be considered as adjuvants for MM immunotherapy.

## METHODS

### Mice

All mice used in this study were on a C57BL/6 genetic background. C57BL/6 WT mice were purchased from the Walter and Eliza Hall Institute for Medical Research (Melbourne, Australia) or bred in-house at QIMR Berghofer Medical Research Institute (Brisbane, Australia). *Id2*<sup>GFP/GFP</sup> mice<sup>64</sup> were kindly provided by Gabrielle Belz (Walter and Eliza Hall Institute for Medical Research, Australia). *Rag1*<sup>-/-</sup>, *Rag2*<sup>-/-</sup> and *Il2rg*<sup>-/-</sup> *Rag2*<sup>-/-</sup> mice have been previously described.<sup>34,65</sup> All mice were bred and maintained at QIMR Berghofer Medical Research Institute and were used at 6–16 weeks of age. Female mice have been used for all experiments except for Figures 1e, f and 7c, e and Supplementary figure 2d–g. *Rag1*<sup>-/-</sup> and *Rag2*<sup>-/-</sup> mice have been alternatively used, depending on availability. All experiments were approved by the QIMR Berghofer Medical Research Institute Animal Ethics Committee.

### Vk\*MYC cell challenge

Experiments with the Vk\*MYC cell lines Vk12653 and Vk12598 were performed as previously described.<sup>33,34</sup> Briefly, Vk\*MYC cells were expanded in *Il2rg*<sup>-/-</sup> *Rag2*<sup>-/-</sup> mice and splenocytes from *Il2rg*<sup>-/-</sup> *Rag2*<sup>-/-</sup> mice containing 40–60% of malignant plasma cells were frozen down and used as a source of Vk\*MYC MM cells. For Vk\*MYC cell challenges, mice were injected intravenously with live splenocytes from *Il2rg*<sup>-/-</sup> *Rag2*<sup>-/-</sup> mice ( $2 \times 10^6$  or  $4 \times 10^5$  cells, for Vk12653 or Vk12598 cell lines, respectively). The presence of monoclonal immunoglobulin (M-protein; quantified as levels of  $\gamma$ -globulin) in the serum was determined by serum protein electrophoresis (HYDRASIS, Sebia Hydragel, Sebia, Inc., Norcross, GA). Percentages and numbers of malignant plasma cells (MM cells) in the spleen and BM were determined by flow cytometry by gating on CD155<sup>+</sup>CD138<sup>+</sup>B220<sup>-</sup> live cells as shown previously.<sup>34</sup> Mice were either killed at a given time point or monitored overtime for external signs of disease

including back-leg paralysis, hunched posture, ruffled fur and swollen abdomen. Sick mice were killed according to a protocol approved by the QIMR Berghofer Medical Research Institute Animal Ethics Committee and in accordance with the National Health and Medical Research Council Guidelines for the Care and Use of Animals for Scientific Purposes.

### ***In vivo* cytokine treatments**

To expand ILC2s, mice received two intraperitoneal injections of 200 ng recombinant mouse IL-33 (BioLegend, Australian Biosearch, Karrinyup, WA, Australia) on days 0 and 2. To induce type 1 immune responses, mice received a single intraperitoneal injection of 200 ng of recombinant mouse IL-12 (BioLegend) together with 200 ng of recombinant mouse IL-18 (Glaxo Smith Kline, King of Prussia, PA, USA). In some experiments, mice received four daily intraperitoneal injections of IL-12 (200 ng) together with IL-18 (200 ng).

### **Flow cytometry**

Single-cell suspensions from mouse spleen, BM, liver, lung or lymph nodes were resuspended in flow cytometry staining buffer containing 2.4G2 (anti-CD16/32) to block Fc receptors. Cell surface staining was performed using conjugated monoclonal Abs (see Supplementary table 1). Dead cells were excluded using live/dead dye Zombie Yellow (BioLegend). The lineage cocktail used included at least TCR $\beta$ , TCR $\gamma\delta$ , CD3, CD19 and CD11c. For some experiments, CD5, CD11b, CD122 and Gr1 were added to the lineage cocktail. For intracellular staining of transcription factors, surface-stained cells were fixed and permeabilized with Foxp3/Transcription Factor Fixation/Fixation kit (eBioscience) and stained with anti-mouse GATA3 (TWAJ; eBioscience, San Diego, CA, USA) or T-bet (4B10; BioLegend). For intracellular cytokine staining, membrane-stained cells were fixed and permeabilized with the BD Cytofix/Cytoperm kit (BD Biosciences) and stained with anti-mouse IL-5 (TRFK5, BioLegend) or IL-13 (eBio13A; eBioscience). Cell numbers were determined using BD Liquid Counting Beads (BD Biosciences), according to the manufacturer's instructions. Samples were acquired on an LSRFortessa 4 lasers flow cytometer (BD Biosciences) and analyzed with FlowJo version 10 (Tree Star).

### **Cell sorting**

BM ILC2s were purified from *Id2*<sup>GFP/GFP</sup> mice. Briefly, BM cell suspensions obtained from the mouse femurs, tibiae and pelvis were stained with anti-CD127-biotin Abs (A7R34; BioLegend) and incubated with streptavidin beads (Miltenyi Biotec) before being positively selected by magnetic-activated cell sorting on MS columns (Miltenyi Biotec). CD127<sup>+</sup>-enriched cells were then stained with anti-lineage (Lin: TCR $\beta$ , TCR $\gamma\delta$ , CD3, CD5, CD11c, CD11b, CD19, CD122 and Gr-1), anti-CD25 and anti-Sca1 monoclonal Abs and Lin<sup>-</sup>GFP<sup>+</sup>CD25<sup>+</sup>Sca1<sup>+</sup> cells were sorted on a BD FACSAria II cell sorter (BD Biosciences, North Ryde, NSW, Australia) with a purity over 95%.

### **Cell culture**

Purified ILC2s were cultured at the density of  $5 \times 10^3$  to  $2 \times 10^6$  cells per well in 96-well plates. Cells were cultured in Roswell Park Memorial Institute-1640 medium (Gibco, Waltham, MA, USA) containing 10% fetal calf serum, 2 mM glutamine, 100 U mL<sup>-1</sup> penicillin, 100 mg mL<sup>-1</sup> streptomycin and 50 mM 2-mercaptoethanol. To promote ILC2 survival and activation, medium was supplemented with IL-2 (20–40 ng mL<sup>-1</sup>) and IL-33 (20–40 ng mL<sup>-1</sup>). In some experiments, IL-12 (1 ng mL<sup>-1</sup>) and IL-18 (20 ng mL<sup>-1</sup>) were added to the cultures.

### **Cytokine analysis**

Cytokine levels in mouse sera or culture supernatants were measured using a Cytometric Bead Array kit (BD Biosciences) according to the manufacturer's instructions. Levels of TSLP, IL-25 or IL-33 in the culture supernatants were measured by ELISA. For TSLP measurement, the assay was performed in 96-well NUNC MaxiSorp plates. TSLP standards and anti-TSLP coating (clone 28F12) and capture (clone 65B12) Abs were purchased from BioLegend. IL-25 and IL-33 were measured using the ELISA-ready-SET-Go! kits from Affymetrix eBioscience according to the manufacturer's instructions.

### **Statistical analyses**

Statistical analyses were carried out using the GraphPad Prism software (San Diego, Ca, USA). For data presented on a log scale (MM cell numbers), statistical analyses were performed on the log-transformed data with the indicated test. Two-sample analyses were performed using either a Mann–Whitney *U*-test or an unpaired *t*-test. Group analyses were performed with a Kruskal–Wallis test followed by a Dunn's multiple comparison *post hoc* test or with a two-way ANOVA followed by a Tukey's multiple comparison *post hoc* test. A log-rank test was used for survival analyses. The Pearson *r* correlation coefficient was calculated to assess correlation between two parameters.

### **ACKNOWLEDGMENTS**

The authors thank Liam Town and Kate Elder for breeding, genotyping, maintenance and care of the mice used in this study. We thank the animal house and flow cytometry facilities at QIMR Berghofer Medical Research Institute. We thank Dr Cyril Seillet for helpful suggestions and discussion. This work was funded by a grant (No. 1122183) awarded to CG through the Priority-driven Collaborative Cancer Research Scheme and cofunded by Cancer Australia, Cure Cancer Australia and Can Too Foundation and by a National Health and Medical Research Council (NHMRC) Program Grant (No. 1132519) and Project Grant (No. 1098960) to MJS and MWLT. CG was supported by an NHMRC of Australia Early Career Fellowship (No. 1107417). KN was supported by the Naito Foundation and NHMRC Project Grant (No. 1159593). MJS and GTB were supported by a Senior Principal Research Fellowship (Nos 1078671 and 1135898,

respectively). CE was supported by an NHMRC Program Grant (No. 1132975) and Fellowship (No. 1154265).

## AUTHOR CONTRIBUTION

**Camille Guillerey:** Conceptualization; Data curation; Formal analysis; Funding acquisition; Investigation; Methodology; Supervision; Writing-original draft. **Kimberley Stannard:** Investigation; Methodology. **Jason Chen:** Investigation; Methodology. **Sophie Krumeich:** Investigation; Methodology. **Kim Miles:** Investigation; Methodology. **Kyohei Nakamura:** Conceptualization; Investigation; Methodology; Writing-review & editing. **Jessica Smith:** Investigation. **Yuan Yu:** Investigation. **Susanna Ng:** Conceptualization. **Heidi Harjunpää:** Investigation. **Michele WL Teng:** Supervision; Writing-review & editing. **Christian Engwerda:** Conceptualization; Supervision; Writing-review & editing. **Gabrielle T Belz:** Resources; Writing-review & editing. **Mark J Smyth:** Conceptualization; Funding acquisition; Resources; Supervision; Writing-review & editing.

## CONFLICT OF INTEREST

MJS has research agreements with Bristol Myers Squibb and Tizona Therapeutics. All other authors declare that they have no conflict of interest.

## REFERENCES

- Jacquelot N, Luong K, Seillet C. Physiological regulation of innate lymphoid cells. *Front Immunol* 2019; **10**: 405.
- Ebihara T, Taniuchi I. Transcription factors in the development and function of group 2 innate lymphoid cells. *Int J Mol Sci* 2019; **20**: 1377.
- Krabbendam L, Bal SM, Spits H, Golebski K. New insights into the function, development, and plasticity of type 2 innate lymphoid cells. *Immunol Rev* 2018; **286**: 74–85.
- Guillerey C. Roles of cytotoxic and helper innate lymphoid cells in cancer. *Mamm Genome* 2018; **29**: 777–789.
- Trabanelli S, Chevalier MF, Derre L, Jandus C. The pro- and anti-tumor role of ILC2s. *Semin Immunol* 2019; **41**: 101276.
- Jovanovic IP, Pejnovic NN, Radosavljevic GD, *et al.* Interleukin-33/ST2 axis promotes breast cancer growth and metastases by facilitating intratumoral accumulation of immunosuppressive and innate lymphoid cells. *Int J Cancer* 2014; **134**: 1669–1682.
- Chevalier MF, Trabanelli S, Racle J, *et al.* ILC2-modulated T cell-to-MDSC balance is associated with bladder cancer recurrence. *J Clin Invest* 2017; **127**: 2916–2929.
- Long A, Dominguez D, Qin L, *et al.* Type 2 Innate lymphoid cells impede IL-33-mediated tumor suppression. *J Immunol* 2018; **201**: 3456–3464.
- Kim J, Kim W, Moon UJ, *et al.* Intratumorally establishing type 2 innate lymphoid cells blocks tumor growth. *J Immunol* 2016; **196**: 2410–2423.
- Saranchova I, Han J, Zaman R, *et al.* Type 2 innate lymphocytes actuate immunity against tumours and limit cancer metastasis. *Sci Rep* 2018; **8**: 2924.
- Ikutani M, Yanagibashi T, Ogasawara M, *et al.* Identification of innate IL-5-producing cells and their role in lung eosinophil regulation and antitumor immunity. *J Immunol* 2012; **188**: 703–713.
- Moral JA, Leung J, Rojas LA, *et al.* ILC2s amplify PD-1 blockade by activating tissue-specific cancer immunity. *Nature* 2020; **579**: 130–135.
- Martinez-Gonzalez I, Matha L, Steer CA, Ghaedi M, Poon GF, Takei F. Allergen-experienced group 2 innate lymphoid cells acquire memory-like properties and enhance allergic lung inflammation. *Immunity* 2016; **45**: 198–208.
- von Moltke J, Ji M, Liang HE, Locksley RM. Tuft-cell-derived IL-25 regulates an intestinal ILC2-epithelial response circuit. *Nature* 2016; **529**: 221–225.
- Kim BS, Siracusa MC, Saenz SA, *et al.* TSLP elicits IL-33-independent innate lymphoid cell responses to promote skin inflammation. *Sci Transl Med* 2013; **5**: 170ra116.
- Ricardo-Gonzalez RR, Van Dyken SJ, Schneider C, *et al.* Tissue signals imprint ILC2 identity with anticipatory function. *Nat Immunol* 2018; **19**: 1093–1099.
- Gury-BenAri M, Thaiss CA, Serafini N, *et al.* The spectrum and regulatory landscape of intestinal innate lymphoid cells are shaped by the microbiome. *Cell* 2016; **166**: 1231–1246.e13.
- Huang Y, Guo L, Qiu J, *et al.* IL-25-responsive, lineage-negative KLRG1(hi) cells are multipotential 'inflammatory' type 2 innate lymphoid cells. *Nat Immunol* 2015; **16**: 161–169.
- Flamar AL, Klose CSN, Moeller JB, *et al.* Interleukin-33 induces the enzyme tryptophan hydroxylase 1 to promote inflammatory group 2 Innate lymphoid cell-mediated immunity. *Immunity* 2020; **52**: 606–619.e6.
- Silver JS, Kearley J, Copenhaver AM, *et al.* Inflammatory triggers associated with exacerbations of COPD orchestrate plasticity of group 2 innate lymphoid cells in the lungs. *Nat Immunol* 2016; **17**: 626–635.
- Ohne Y, Silver JS, Thompson-Snipes L, *et al.* IL-1 is a critical regulator of group 2 innate lymphoid cell function and plasticity. *Nat Immunol* 2016; **17**: 646–655.
- Bal SM, Bernink JH, Nagasawa M, *et al.* IL-1 $\beta$ , IL-4 and IL-12 control the fate of group 2 innate lymphoid cells in human airway inflammation in the lungs. *Nat Immunol* 2016; **17**: 636–645.
- Afferri C, Buccione C, Andreone S, *et al.* The pleiotropic immunomodulatory functions of IL-33 and Its implications in tumor immunity. *Front Immunol* 2018; **9**: 2601.
- Villarreal DO, Wise MC, Walters JN, *et al.* Alarmin IL-33 acts as an immunoadjuvant to enhance antigen-specific tumor immunity. *Cancer Res* 2014; **74**: 1789–1800.
- Smithgall MD, Comeau MR, Yoon BR, Kaufman D, Armitage R, Smith DE. IL-33 amplifies both Th1- and Th2-type responses through its activity on human basophils, allergen-reactive Th2 cells, iNKT and NK cells. *Int Immunol* 2008; **20**: 1019–1030.

26. Bourgeois E, Van LP, Samson M, et al. The pro-Th2 cytokine IL-33 directly interacts with invariant NKT and NK cells to induce IFN- $\gamma$  production. *Eur J Immunol* 2009; **39**: 1046–1055.
27. Lim HX, Choi S, Cho D, Kim TS. IL-33 inhibits the differentiation and immunosuppressive activity of granulocytic myeloid-derived suppressor cells in tumor-bearing mice. *Immunol Cell Biol* 2017; **95**: 99–107.
28. Qin L, Dominguez D, Chen S, et al. Exogenous IL-33 overcomes T cell tolerance in murine acute myeloid leukemia. *Oncotarget* 2016; **7**: 61069–61080.
29. Villarreal DO, Weiner DB. IL-33 isoforms: their future as vaccine adjuvants? *Expert Rev Vaccines* 2015; **14**: 489–492.
30. Fournie JJ, Poupot M. The Pro-tumorigenic IL-33 involved in antitumor immunity: a yin and yang cytokine. *Front Immunol* 2018; **9**: 2506.
31. Halim TY, MacLaren A, Romanish MT, Gold MJ, McNagny KM, Takei F. Retinoic-acid-receptor-related orphan nuclear receptor alpha is required for natural helper cell development and allergic inflammation. *Immunity* 2012; **37**: 463–474.
32. Hoyler T, Klose CS, Souabni A, et al. The transcription factor GATA-3 controls cell fate and maintenance of type 2 innate lymphoid cells. *Immunity* 2012; **37**: 634–648.
33. Guillerey C, Nakamura K, Pichler AC, et al. Chemotherapy followed by anti-CD137 mAb immunotherapy improves disease control in a mouse myeloma model. *JCI Insight* 2019; **5**: e125932.
34. Guillerey C, Ferrari de Andrade L, Vuckovic S, et al. Immunosurveillance and therapy of multiple myeloma are CD226 dependent. *J Clin Invest* 2015; **125**: 2077–2089.
35. Laffont S, Blanquart E, Savignac M, et al. Androgen signaling negatively controls group 2 innate lymphoid cells. *J Exp Med* 2017; **214**: 1581–1592.
36. Wagner M, Moro K, Koyasu S. Plastic heterogeneity of innate lymphoid cells in cancer. *Trends Cancer* 2017; **3**: 326–335.
37. Kadel S, Ainsua-Enrich E, Hatipoglu I, et al. A major population of functional KLRG1<sup>-</sup> ILC2s in female lungs contributes to a sex bias in ILC2 Numbers. *Immunohorizons* 2018; **2**: 74–86.
38. Cephus JY, Stier MT, Fuseini H, et al. Testosterone attenuates group 2 innate lymphoid cell-mediated airway inflammation. *Cell Rep* 2017; **21**: 2487–2499.
39. Nussbaum JC, Van Dyken SJ, von Moltke J, et al. Type 2 innate lymphoid cells control eosinophil homeostasis. *Nature* 2013; **502**: 245–248.
40. Guillerey C, Smyth MJ. NK cells and cancer immunoediting. *Curr Top Microbiol Immunol* 2016; **395**: 115–145.
41. Putz EM, Guillerey C, Kos K, et al. Targeting cytokine signaling checkpoint CIS activates NK cells to protect from tumor initiation and metastasis. *Oncoimmunology* 2017; **6**: e1267892.
42. TrabANELLI S, Chevalier MF, Martinez-Usatorre A, et al. Tumour-derived PGD2 and Nkp30-B7H6 engagement drives an immunosuppressive ILC2-MDSC axis. *Nat Commun* 2017; **8**: 593.
43. TrabANELLI S, Curti A, Lecciso M, et al. CD127<sup>+</sup> innate lymphoid cells are dysregulated in treatment naive acute myeloid leukemia patients at diagnosis. *Haematologica* 2015; **100**: e257–e260.
44. Hildreth AD, O’Sullivan TE. Tissue-resident innate and innate-like lymphocyte responses to viral infection. *Viruses* 2019; **11**.
45. Blimark C, Holmberg E, Mellqvist UH, et al. Multiple myeloma and infections: a population-based study on 9253 multiple myeloma patients. *Haematologica* 2015; **100**: 107–113.
46. Guillerey C, Nakamura K, Vuckovic S, Hill GR, Smyth MJ. Immune responses in multiple myeloma: role of the natural immune surveillance and potential of immunotherapies. *Cell Mol Life Sci* 2016; **73**: 1569–1589.
47. Taylor S, Huang Y, Mallett G, et al. PD-1 regulates KLRG1<sup>+</sup> group 2 innate lymphoid cells. *J Exp Med* 2017; **214**: 1663–1678.
48. Paiva B, Azpilikueta A, Puig N, et al. PD-L1/PD-1 presence in the tumor microenvironment and activity of PD-1 blockade in multiple myeloma. *Leukemia* 2015; **29**: 2110–2113.
49. Gasteiger G, Fan X, Dikiy S, Lee SY, Rudensky AY. Tissue residency of innate lymphoid cells in lymphoid and nonlymphoid organs. *Science* 2015; **350**: 981–985.
50. Huang Y, Mao K, Chen X, et al. S1P-dependent interorgan trafficking of group 2 innate lymphoid cells supports host defense. *Science* 2018; **359**: 114–119.
51. Mjosberg JM, Trifari S, Crellin NK, et al. Human IL-25- and IL-33-responsive type 2 innate lymphoid cells are defined by expression of CRTH2 and CD161. *Nat Immunol* 2011; **12**: 1055–1062.
52. Steinmann S, Schoedsack M, Heinrich F, et al. Hepatic ILC2 activity is regulated by liver inflammation-induced cytokines and effector CD4<sup>+</sup> T cells. *Sci Rep* 2020; **10**: 1071.
53. Stier MT, Zhang J, Goleniewska K, et al. IL-33 promotes the egress of group 2 innate lymphoid cells from the bone marrow. *J Exp Med* 2018; **215**: 263–281.
54. Schneider C, Lee J, Koga S, et al. Tissue-resident group 2 innate lymphoid cells differentiate by layered ontogeny and in situ perinatal priming. *Immunity* 2019; **50**: 1425–1438.e1425.
55. Germain RN, Huang YF. ILC2s-resident lymphocytes pre-adapted to a specific tissue or migratory effectors that adapt to where they move? *Curr Opin Immunol* 2019; **56**: 76–81.
56. Zhang Y, Qi C, Li L, et al. CD8<sup>+</sup> T cell/IL-33/ILC2 axis exacerbates the liver injury in Con A-induced hepatitis in T cell-transferred Rag2-deficient mice. *Inflamm Res* 2019; **68**: 75–91.
57. McHedlidze T, Waldner M, Zopf S, et al. Interleukin-33-dependent innate lymphoid cells mediate hepatic fibrosis. *Immunity* 2013; **39**: 357–371.
58. Martinez-Gonzalez I, Ghaedi M, Steer CA, Matha L, Vivier E, Takei F. ILC2 memory: recollection of previous activation. *Immunol Rev* 2018; **283**: 41–53.
59. Shankaran V, Ikeda H, Bruce AT, et al. IFN $\gamma$  and lymphocytes prevent primary tumour development and shape tumour immunogenicity. *Nature* 2001; **410**: 1107–1111.

60. Zheng X, Turkowski K, Mora J, *et al.* Redirecting tumor-associated macrophages to become tumoricidal effectors as a novel strategy for cancer therapy. *Oncotarget* 2017; **8**: 48436–48452.
61. Schindler H, Lutz MB, Rollinghoff M, Bogdan C. The production of IFN- $\gamma$  by IL-12/IL-18-activated macrophages requires STAT4 signaling and is inhibited by IL-4. *J Immunol* 2001; **166**: 3075–3082.
62. Komai-Koma M, Wang E, Kurowska-Stolarska M, Li D, McSharry C, Xu D. Interleukin-33 promoting Th1 lymphocyte differentiation depends on IL-12. *Immunobiology* 2016; **221**: 412–417.
63. Yang Q, Li G, Zhu Y, *et al.* IL-33 synergizes with TCR and IL-12 signaling to promote the effector function of CD8<sup>+</sup> T cells. *Eur J Immunol* 2011; **41**: 3351–3360.
64. Rankin LC, Groom JR, Chopin M, *et al.* The transcription factor T-bet is essential for the development of NKp46<sup>+</sup> innate lymphocytes via the Notch pathway. *Nat Immunol* 2013; **14**: 389–395.
65. Andrews DM, Smyth MJ. A potential role for RAG-1 in NK cell development revealed by analysis of NK cells during ontogeny. *Immunol Cell Biol* 2010; **88**: 107–116.

## SUPPORTING INFORMATION

Additional supporting information may be found online in the Supporting Information section at the end of the article.

© 2020 Australian and New Zealand Society for Immunology Inc.